



**HAL**  
open science

## Mapping Cellular Polarity Networks Using Mass Spectrometry-based Strategies

Avais M Daulat, Tania Puvirajesinghe, Luc Camoin, Jean-Paul Borg

► **To cite this version:**

Avais M Daulat, Tania Puvirajesinghe, Luc Camoin, Jean-Paul Borg. Mapping Cellular Polarity Networks Using Mass Spectrometry-based Strategies. *Journal of Molecular Biology*, 2018, 430 (19), pp.3545-3564. <10.1016/j.jmb.2018.05.023>. <hal-02145872>

**HAL Id: hal-02145872**

**<https://hal.science/hal-02145872v1>**

Submitted on 3 Jun 2019

**HAL** is a multi-disciplinary open access archive for the deposit and dissemination of scientific research documents, whether they are published or not. The documents may come from teaching and research institutions in France or abroad, or from public or private research centers.

L'archive ouverte pluridisciplinaire **HAL**, est destinée au dépôt et à la diffusion de documents scientifiques de niveau recherche, publiés ou non, émanant des établissements d'enseignement et de recherche français ou étrangers, des laboratoires publics ou privés.



HAL Authorization

1 **Mapping cellular polarity networks using mass spectrometry-based strategies**

2  
3  
4  
5 3 Avais. M. Daulat<sup>1,\* #</sup>, Tania M. Puvirajasinghe<sup>1,\*</sup>, Luc Camoin<sup>2</sup>, and Jean-Paul Borg<sup>1,2#</sup>  
6  
7  
8 4  
9  
10 5  
11  
12  
13 6  
14  
15

16 7 <sup>1</sup> Centre de Recherche en Cancérologie de Marseille (CRCM), 'Cell Polarity, Cell  
17 8 Signalling, and Cancer', Equipe Labellisée Ligue Contre le Cancer, Aix Marseille  
19 9 Univ, CNRS, INSERM, Institut Paoli-Calmettes, CRCM, Marseille, France. <sup>2</sup> Aix  
21 10 Marseille Univ, CNRS, INSERM, Institut Paoli-Calmettes, CRCM, 'Marseille  
23 11 proteomics', Marseille, France.  
24  
25  
26 12  
27  
28  
29 13  
30

31 14 \* Co-first authors

32  
33  
34 15 #corresponding authors: jean-paul.borg@inserm.fr (J.-P. Borg) and  
35  
36 16 avais.daulat@inserm.fr (A. M Daulat)  
37  
38  
39 17  
40  
41

42 18 **Abbreviations**

43  
44  
45 19 aPKC, atypical protein kinase C; APEX, engineered ascorbate peroxidase; BioID,  
46 20 proximity-dependent biotin identification; Dlg, Discs Large; (FERM)-binding motif  
47  
48 21 (FBM); GST, glutathione S-transferase, HRP, horseradish peroxidase; Lgl, Lethal  
49  
50 22 Giant Larva; MAGUK, membrane-associated guanylate kinase; MS/MS, mass  
51  
52 23 spectrometry; MST1/2, microtubule affinity-regulating kinases 1/2; PATJ, Pals1-  
53  
54 24 associated tight junction protein; PCP, Planar Cell Polarity; PDZBM, PDZ binding  
55  
56  
57  
58  
59  
60  
61  
62  
63  
64  
65

25 motif; LRR, leucine-rich repeat; Stdt, Stardust; STRAD, STe-20 Related ADaptor;  
26 Tobacco Etch Virus (TEV) protease; Yeast-2 hybrid (Y2H).

## 27 **Abstract**

28 Cell polarity is a vital biological process involved in the building, maintenance and  
29 normal functioning of tissues in invertebrates and vertebrates. Unsurprisingly,  
30 molecular defects affecting polarity organization and functions have a strong impact  
31 on tissue homeostasis, embryonic development and adult life, and may directly or  
32 indirectly lead to diseases. Genetic studies have demonstrated the causative effect of  
33 several polarity genes in diseases, however much remains to be clarified before a  
34 comprehensive view of the molecular organization and regulation of the protein  
35 networks associated with polarity proteins is obtained. This challenge can be  
36 approached head-on using proteomics to identify protein complexes involved in cell  
37 polarity and their modifications in a spatio-temporal manner. We review the  
38 fundamental basics of mass spectrometry techniques and provide an in-depth  
39 analysis of how mass spectrometry has been instrumental in understanding the  
40 complex and dynamic nature of some cell polarity networks at the tissue (apico-basal  
41 and planar cell polarities) and cellular (cell migration, ciliogenesis) levels, with the fine  
42 dissection of the interconnections between prototypic cell polarity proteins and signal  
43 transduction cascades in normal and pathological situations. This review primarily  
44 focuses on epithelial structures which are the fundamental building blocks for most  
45 metazoan tissues, used as the archetypal model to study cellular polarity. This field  
46 offers broad perspectives thanks to the ever-increasing sensitivity of mass  
47 spectrometry and its use in combination with recently developed molecular strategies  
48 able to probe *in situ* proteomic networks.

## 49 Introduction

1  
2  
3 50 Epithelial cells form complex tridimensional structures acting not only as barriers  
4  
5 51 against external physical, chemical and biological threats but also as filters allowing  
6  
7  
8 52 the regulated transport of nutriments between the internal and external compartments  
9  
10 53 of the organism. During tissue and organ morphogenesis, epithelial cells adhere to  
11  
12  
13 54 neighboring cells and to the supporting substrates, and adopt a highly organized  
14  
15 55 structure with an apical domain in contact with the external environment. Apico-basal  
16  
17  
18 56 polarity describes the underlying molecular mechanisms of this lateral axis  
19  
20 57 organization, and has been studied for several decades from the molecular,  
21  
22  
23 58 functional and genetic viewpoints, in a plethora of organisms. Epithelial cell  
24  
25 59 membranes are divided into apical and basolateral compartments which are  
26  
27  
28 60 segregated by adherens (AJs) and tight (TJs) junctions formed by complex networks  
29  
30 61 of cell adhesion molecules, intracellular adaptors, enzymes and cytoskeletal proteins  
31  
32 62 (FIGURE 1A) <sup>1</sup>. Cell junctions are made of cell surface core components such as E-  
33  
34  
35 63 cadherin in AJs and claudins and occludin in TJs, which are associated with  
36  
37 64 intracellular machineries connecting these membrane structures to the cytoskeleton  
38  
39  
40 65 and signaling networks. This finely tuned apico-basal axis orientation is organized  
41  
42 66 and maintained by a set of asymmetrically distributed polarity protein complexes  
43  
44 67 which have mainly been identified by genetic screens <sup>2; 3</sup>. Studies in *Drosophila*  
45  
46  
47 68 *melanogaster* have indeed pinpointed three evolutionarily conserved polarity  
48  
49 69 complexes, the PAR (partitioning defective), CRUMBS and SCRIB complexes <sup>4</sup>  
50  
51  
52 70 which localize apically (PAR, CRUMBS) or basolaterally (SCRIB) and act  
53  
54 71 antagonistically to maintain apico-basal polarity in the fly (FIGURE 1B) <sup>5</sup>. Each  
55  
56  
57 72 complex is composed of multiple subunits containing PDZ domain containing proteins  
58  
59 73 acting as scaffolding molecules (PAR-3, PAR-6, SCRIB, Stardust, Discs Large),  
60  
61  
62  
63  
64  
65

1  
2  
3  
4  
5  
6  
7  
8  
9  
10  
11  
12  
13  
14  
15  
16  
17  
18  
19  
20  
21  
22  
23  
24  
25  
26  
27  
28  
29  
30  
31  
32  
33  
34  
35  
36  
37  
38  
39  
40  
41  
42  
43  
44  
45  
46  
47  
48  
49  
50  
51  
52  
53  
54  
55  
56  
57  
58  
59  
60  
61  
62  
63  
64  
65

74 small GTPases (CDC42) and protein kinases (atypical PKC, aPKC). The Par  
75 complex is the best characterized of these complexes at the molecular level; it  
76 contains the PAR-3 and PAR-6 PDZ proteins, and aPKC <sup>1</sup>. Other PDZ proteins  
77 (PAR-6, MAGUKs) bind to the cell surface molecule Crumbs, the major component of  
78 another cell polarity complex, through a well conserved carboxyl-terminal PDZ  
79 binding motif (PDZBM)<sup>6</sup>. The SCRIB complex is genetically described as having a  
80 causative role in apico-basal polarity and epithelial homeostasis in *Drosophila*.  
81 Several components of this complex (i.e. SCRIB, Discs Large (DLG), and Lethal  
82 Giant Larvae (LGL)) behave as strong tumor suppressor genes<sup>3; 7; 8</sup> and are  
83 evolutionarily conserved, from invertebrates to humans. The exact molecular  
84 composition of the PAR and SCRIB complexes were later studied using proteomic-  
85 based strategies which will be described in this review.

86 Planar Cell Polarity (PCP) is the second major, though more poorly characterized  
87 process, organizing epithelial sheets and their apical structures perpendicular to the  
88 apico-basal axis (FIGURE 1A). The importance of this cellular program is  
89 demonstrated by mutations in PCP genes which disrupt the stereotyped hair  
90 orientation on *Drosophila* wings and the alignment of the stereocilia in the mouse  
91 inner ear. Genetic studies initially performed in *Drosophila* identified a set of core  
92 PCP genes responsible for the establishment of planar cell polarity <sup>9</sup>. These genes  
93 encode integral membrane molecules such as Frizzled, Van Gogh, Flamingo as well  
94 as cytoplasmic proteins such as Dishevelled, Prickle and Diego. In the *Drosophila*  
95 epithelial system, core PCP proteins have a strikingly asymmetrical distribution in  
96 cells along a proximal-distal gradient. The protein complex comprising Van Gogh,  
97 Flamingo and Prickle is localized at the proximal sides whereas Frizzled, Flamingo,  
98 Dishevelled and Diego proteins are localized at the distal sides (FIGURE 1C). During

1  
2  
3  
4  
5  
6  
7  
8  
9  
10  
11  
12  
13  
14  
15  
16  
17  
18  
19  
20  
21  
22  
23  
24  
25  
26  
27  
28  
29  
30  
31  
32  
33  
34  
35  
36  
37  
38  
39  
40  
41  
42  
43  
44  
45  
46  
47  
48  
49  
50  
51  
52  
53  
54  
55  
56  
57  
58  
59  
60  
61  
62  
63  
64  
65

99 early gastrulation, a subset of core PCP molecules controls a phenomenon called  
100 convergent-extension which contributes to the formation of the antero-posterior axis  
101 of the embryo<sup>10</sup>. In addition to the crucial role of PCP in the correct execution of  
102 developmental events, increasing numbers of studies detail its importance in the  
103 proper organization and function of adult tissues and organs. Likewise, loss-of-  
104 function mutations in PCP genes lead to multiple diseases including neural tube  
105 defects<sup>11</sup> and polycystic kidney disease<sup>12</sup>. Recently, downregulation or, more  
106 frequently, upregulation of PCP genes has been associated with cancer progression  
107 either by promoting growth, resistance to cell death and drug treatment, or  
108 metastasis<sup>13</sup>.

109 Much of the knowledge and understanding of apico-basal and planar cell polarities  
110 has been obtained through genetic screens, mainly in invertebrates (*D.*  
111 *melanogaster*, *C. elegans*). This led to the discovery of master genes devoted to the  
112 establishment and maintenance of epithelial polarities, and has highlighted how cell  
113 polarity defects can have a strong impact in cellular, tissue, and organ and organism  
114 homeostasis. A deeper understanding of these cellular programs has been obtained  
115 using protein-based strategies, especially to identify protein associated networks, but  
116 also the post-translational regulation of cell polarity proteins.

117 Over the last decade, mass spectrometry has been critical in elucidating new polarity  
118 protein components and complexes, as well as in revealing unexpected modes of  
119 action of these proteins. Various strategies have been used over the years to prepare  
120 samples for mass spectrometry analysis in order to purify high quality protein  
121 complexes amenable to mass spectrometry analysis. Sample preparation methods  
122 are largely dictated by the biological question addressed, which we will detail in the  
123 review. One of the main advantages of mass spectrometry is that the functional

124 hypothesis is no longer answered by a binary yes/no response, but by a multi-  
125 dimensional response. Unlike genetic methods and yeast two-hybrid assays, which  
126 test the direct interaction between a specific bait with a partner (prey), proteomics  
127 analysis provides more complex information.

128 This review describes how mass spectrometry has contributed to identify apico-basal  
129 and planar cell polarities networks, as well as other molecular networks involved in  
130 cell polarity processes occurring at the cellular level during cell migration and  
131 ciliogenesis. This review is organized in sections which focus on the following topics:

- 132 - Basis of mass spectrometry and techniques used to purify and concentrate  
133 protein complex populations amenable to mass spectrometry analysis.
- 134 - Specific examples of how mass spectrometry has allowed the molecular  
135 dissection of cell polarity protein networks involved in cell polarity (including  
136 apico-basal polarity, planar cell polarity, cell migration and ciliogenesis).
- 137 - Examples of how mass spectrometry has fueled new fields of research by  
138 connecting different types of cell polarity.

### 140 **Protein identification by mass spectrometry**

141 The term 'proteomics' was created over 25 years ago, with the aim of providing a  
142 complete characterization of all proteins ('proteome') expressed by a given genome  
143<sup>14; 15</sup>. The term 'proteoform' was then used to define a specific molecular form of a  
144 protein product arising from a specific gene (including products differing due to  
145 genetic variations, alternatively spliced RNA, and post-translational modifications)<sup>16</sup>.

146 Proteomics aims to elucidate the properties and functions of proteins by defining their  
1 amino acid sequences, post-translations modifications and protein interactions,  
2 147 amongst other parameters. Ideally, when carried out at a large scale, proteomics  
3  
4 148 offers an integrated view of a complex biological process or cellular network <sup>17</sup>. The  
5  
6 149 human genome contains approximately 20,000 genes, with more than 50% of them  
7  
8 150 giving rise to alternative splice variants. However the total number of proteins  
9  
10 151 expressed, including isoforms produced by splice variants, non-pathological and  
11  
12 152 pathological amino-acid changes and post-translational modifications, is currently  
13  
14 153 greater than 1 million. In addition, the numbers of copies of each protein in the ~230  
15  
16 154 human cell types can range from zero to 10,000,000. The proteome catalyzes and  
17  
18 155 essentially controls all cellular processes and constitutes about 50-60% of the dry  
19  
20 156 mass of a cell. Further layers of complexity are added by cellular processes which  
21  
22 157 modify proteins such as phosphorylation, ubiquitination, degradation, protein  
23  
24 158 localization and protein-protein interactions <sup>18</sup>.  
25  
26  
27  
28  
29  
30  
31  
32  
33

34  
35 160 Mass spectrometry devices measure the mass-to-charge ratio of gas phase ions.  
36  
37 161 Mass spectrometers have three main components, which include an ion source, a  
38  
39 162 mass analyzer, which separates ionized substrates according to their ratio, and a  
40  
41 163 detector. In proteomics applications, two main types of soft ionisation techniques are  
42  
43 164 used to generate protein and peptide ions, which include matrix assisted laser  
44  
45 165 desorption ionization (MALDI) and electro-spray ionization (ESI). Nano-electrospray  
46  
47 166 (nanoES) is the ionization method of choice to generate additional partial sequence  
48  
49 167 information to complement the mass information <sup>19</sup>. The ions follow a trajectory  
50  
51 168 established by the Lorentz force in electric or magnetic field. The electrodynamic ion  
52  
53 169 funnel allows the manipulation and focusing of ions in a pressure regime, which are  
54  
55  
56  
57  
58  
59 170 then analyzed using mass analyzers. Different mass analyzers can be associated  
60  
61  
62  
63  
64  
65

171 with each ionization approach. The mass analyzer is the unit of the mass  
172 spectrometer dedicated to manipulating ionized masses and separating them based  
173 on mass-to-charge ratios, and distributing them to the detector. The main analyzers  
174 used in proteomics are the quadrupole (Q), the time of flight (TOF), the ion-trap (IT)  
175 and the Orbitrap (OB). A technical dissection of the component units of mass  
176 spectrometry devices is provided in the following review <sup>20</sup>. High-throughput  
177 proteomics rely on two main strategies: bottom-up or top-down approaches.

178 All bottom-up proteomics approaches require protein digestion by a sequence-  
179 specific enzyme such as trypsin which cleaves after basic amino acids (lysine or  
180 arginine) (FIGURE 2)<sup>21</sup>. The peptides thus generated are then separated by reverse  
181 phase chromatography, and ionized directly using ESI or indirectly using MALDI,  
182 after which the ionized peptides are introduced into the vacuum of a mass  
183 spectrometer. The ions are manipulated and analyzed using different mass analyzers  
184 such as Q and OB as a quadrupole-orbitrap mass spectrometer (Q-Exactive; Thermo  
185 Scientific). However, other types of mass spectrometers are also used for data  
186 acquisition. Usually the acquisition method used is automated data dependant  
187 acquisition (DDA) also known as tandem mass spectrometry. DDA involves multiple  
188 steps switching from full scan MS which measures the mass-to-charge ratios of  
189 ionized peptides, to a series of MS/MS acquisition according to data dependent  
190 criteria. MS and MS/MS spectrum are then analyzed by softwares (such as  
191 MaxQuant and Perseus software) which identify the peptides <sup>22; 23; 24</sup>. These search  
192 engines attribute each MS and MS/MS spectrum to the peptide of a given protein,  
193 thereby allowing the protein content of the sample to be identified and/or a particular  
194 post-translational modification (PTM) modification to be precisely mapped within a  
195 protein sequence. In targeted proteomics, the DDA is limited to a list of peptides and

196 their fragmented ions. Peptides of known mass-to-charge ratio ( $m/z$ ) (parents ions)  
197 are selected in the first quadrupole, the peptide is then fragmented and several  
198 fragment ions are monitored over time using a quadrupole (for single reaction  
199 monitoring analysis ; SRM) or a high resolution mass analyzer such as an Orbitrap  
200 (for parallel reaction monitoring ; PRM)<sup>25</sup>. These transitions (parent ion / fragment  
201 ions) are multiplexed and their specificity is checked against a spectral library using  
202 dedicated software packages such as SkyLine <sup>26</sup>. A third acquisition method called  
203 data-independent acquisition (DIA) is also available for bottom-up proteomics. DIA is  
204 a method in which all ions within a selected  $m/z$  range (5-25  $m/z$ ) are fragmented and  
205 analyzed all together in MS/MS <sup>25; 27; 28</sup>. This DIA strategy has quickly expanded over  
206 the last few years because of the availability of next-generation mass spectrometers  
207 with high resolution and accurate mass (HR/AM). As for PRM, DIA analysis requires  
208 spectral libraries derived from auxiliary DDA data to provide protein identification and  
209 quantification. New software tools applied to DIA analysis are proposed by different  
210 groups such as Skyline and open SWATH<sup>29</sup>.

211 In contrast, top-down proteomics does not require any prior proteolytic digestion.  
212 Top-down proteomics allows the identification and relative quantification of unique  
213 proteoforms by direct analysis of whole proteins<sup>30</sup>. Proteins are typically ionized by  
214 electrospray ionization and analyzed using HR/AM mass spectrometry for mass  
215 measurement. These whole proteins are then fragmented by direct ion dissociation in  
216 the gas phase using electron-capture dissociation (ECD) or electron-transfer  
217 dissociation (ETD). The main advantages of the top-down approach include the  
218 ability to detect degradation products, sequence variants, and combinations of post-  
219 translational modifications. Software dedicated to top-down proteomics still need to  
220 be developed, except for the ProSightPC initially described by Kelleher team<sup>31</sup>. The

221 main disadvantage of top-down proteomics is its limitation to relative simple mixtures  
1  
2 222 and to small proteins (10-30 kDa). The latter limitation can be overcome using  
3  
4 223 middle-down proteomics which consists in limiting protein digestion in order to yield  
5  
6  
7 224 relatively larger peptides (ideally above 3 kDa). Fewer peptides are generated in  
8  
9  
10 225 comparison to bottom-up proteomics (peptides from 0.7 to 3 kDa); the complexity of  
11  
12 226 the digested products is thus reduced which allows better proteome coverage for  
13  
14 227 proteins of higher molecular weight, which cannot be analysed by top-down  
15  
16  
17 228 proteomics. To date, most of the middle-down proteomics studies have been limited  
18  
19 229 to very specific applications<sup>32</sup>.

230 Given the importance of dynamic regulation of protein expression and the  
231 modifications of proteins, it is crucial to be able to monitor the dynamics of the  
232 proteomes. Different quantitative proteomics approaches have been developed.  
233 Quantitative proteomics is currently mainly based on bottom-up strategies using  
234 DDA, DIA and targeted acquisition. Numerous methods allowing relative as well as  
235 absolute quantification are available. Quantitative proteomics can be performed by  
236 two major approaches: one using stable isotopes and one named the "label-free"  
237 method. Stable isotope-based quantitative proteomics allows the identification of  
238 equivalent peptides using the specific increase in mass due to the addition of mass  
239 tags with stable isotopes as <sup>13</sup>C, <sup>15</sup>N and <sup>18</sup>O. Several strategies (ICAT, ICPL, iTRAQ,  
240 TMT, SILAC) involving stable isotopes have been developed using metabolic or  
241 chemical labelling<sup>33</sup>. The classical workflow consists of mixing labelled samples  
242 containing the heavy mass tags and the light samples with no tags. The relative  
243 abundance of peptides and proteins is revealed at the MS level (ICAT, ICPL, SILAC,  
244 AQUA) or at the MS/MS level (iTRAQ, TMT). Alternatively, the quantitative  
245 proteomics approach named "label-free" allows the relative abundance of proteins to

246 be determined between several samples and/or conditions by directly measuring the  
1  
2 247 difference of abundance of different peptides/proteins by LC-MS/MS. This method is  
3  
4  
5 248 based on the measurement of the spectral intensities of the precursor ions in MS and  
6  
7 249 the integration of these intensities through the chromatographic elution profile. This  
8  
9  
10 250 approach is possible thanks to the remarkable improvements of mass spectrometry  
11  
12 251 devices over the last few years and to the strong correlation between the intensities  
13  
14 252 of the ions and their abundance in the process of ionization by electrospray. The  
15  
16  
17 253 'label-free' method requires a good precision of the detected masses, an important  
18  
19 254 spectral resolution and precise and reproducible times of retention for the eluted  
20  
21  
22 255 peptides. The relative abundance of peptides and proteins is revealed at the MS level  
23  
24 256 and the identification at the MS/MS level. A large number of softwares are available  
25  
26 257 for "label-free" proteomics analysis. The most popular ones are MaxQuant developed  
27  
28  
29 258 by J. Cox and M. Mann <sup>22; 24</sup> and Progenesis QI (Waters). In targeted proteomics,  
30  
31 259 SRM, PRM and DIA, absolute quantification methods use synthetic AQUA peptides  
32  
33  
34 260 in which amino acids containing stable isotopes are incorporated into the peptide.  
35  
36 261 AQUA peptides are used as internal standards allowing the absolute quantification of  
37  
38  
39 262 proteins<sup>34</sup>. FIGURE 2 depicts the main steps of sample preparation for mass  
40  
41 263 spectrometry analysis. Over the past two decades, several strategies have been  
42  
43  
44 264 used to purify protein complexes amenable to mass spectrometry analysis. These  
45  
46 265 strategies each have their specific advantages and limitations, which we will describe  
47  
48  
49 266 in the following sections and is summarized in (TABLE 1).

### 267 **Purifying protein complexes using peptide pull down strategies**

268 The peptide pull-down technique is commonly used to identify interactions occurring  
269 on a limited sequence of a protein of interest. Synthetic peptides or recombinant  
270 protein fragments mimicking the sequence of interest used as baits are fused for

271 example to glutathione S-transferase (GST)) or not and subsequently bound  
272 covalently or non-covalently to agarose beads. Peptide pull-down strategies have  
273 been extensively used for intracellular sequences of membrane proteins<sup>35; 36</sup> the  
274 purification of which in large quantities is difficult due to low expression levels and  
275 poor solubility<sup>37</sup>. Peptides can be synthesized with biotin modifications and  
276 subsequently precipitated with streptavidin beads to purify proteins from cell lysates  
277 and identify interacting proteins<sup>38</sup>. This method allows the rapid identification of  
278 interactors; however it is limited to peptides and relies on limited linear motives.  
279 Peptide pull-down methods have for instance been used for the identification of  
280 protein interactors of the cytosolic regions of membrane proteins such as G protein–  
281 coupled receptors (GPCRs)<sup>36</sup>. Another advantage of this approach is the possibility  
282 to easily generate a mutant for a specific binding domain. For example, PDZ domains  
283 bind to a three amino acid hydrophobic motif generally found at the C-terminus of  
284 proteins. Mutation of this motif usually leads to a complete loss of interaction with  
285 PDZ domains. Using a peptide encompassing the C-terminus of VANGL2, it has  
286 been possible to identify two PDZ domain-containing proteins, SCRIB and SNX27,  
287 the interaction of which is disrupted with the mutant peptide<sup>38</sup>.

## 288 **Tandem Affinity Purification tag (TAP-tag) of Proteins**

289 In 1999, Bertrand Séraphin's group designed a novel method to purify protein  
290 complexes under native conditions<sup>39</sup>. This protocol has been extensively used in  
291 yeast<sup>40</sup> and later in human cells focusing on TNF $\alpha$ /NF- $\kappa$ B signaling<sup>41</sup>. The tag  
292 consists of two IgG binding domains followed by a calmodulin binding domain,  
293 separated by a site of recognition for the Tobacco Etch Viruses (TEV) protease. This  
294 two-step purification method allows the rapid purification of proteins complexes under  
295 native conditions with low amount of background proteins. Despite the versatility of

1  
2  
3  
4  
5  
6  
7  
8  
9  
10  
11  
12  
13  
14  
15  
16  
17  
18  
19  
20  
21  
22  
23  
24  
25  
26  
27  
28  
29  
30  
31  
32  
33  
34  
35  
36  
37  
38  
39  
40  
41  
42  
43  
44  
45  
46  
47  
48  
49  
50  
51  
52  
53  
54  
55  
56  
57  
58  
59  
60  
61  
62  
63  
64  
65

296 the TAP-tag protocol, the size of the tag (~25kDa) may hinder some interactions. For  
297 this reason, several groups have optimized the original protocol by developing  
298 various combinations of tags to reduce the hindrance of the tag. One example is a  
299 combination of two streptavidin binding domains followed by a calmodulin binding  
300 domain (~10kDa), which has been successfully used to decipher the molecular  
301 mechanisms of Wnt and Sonic Hedgehog signaling pathways<sup>42; 43</sup>.

### 302 **Single-step protein purification**

303 Over the last ten years, mass spectrometry has become increasingly sophisticated  
304 and has allowed the development of novel purification methods. For example, several  
305 groups have used Flag-tagged proteins<sup>44; 45</sup> to identify weakly expressed proteins  
306 and their associated protein complexes and to characterize proteins complexes with  
307 lower affinity. This strategy however yields a high rate of false positive hits, which can  
308 be identified as such and disregarded if appropriate controls are used. A list of the  
309 common “contaminant” proteins (<http://crapome.org/>) has been generated and can be  
310 used to rapidly discriminate false positives from real partners<sup>46</sup>. The advantages of  
311 the single-step purification methods are the small size of the tag, which limits steric  
312 hindrance for interacting proteins, as well as the rapidity of the purification compared  
313 to TAP-tag protocol, thus circumventing the use of time-consuming techniques which  
314 may lead to a loss of associated proteins.

315 Due to the recent emergence of nanobody technology and the availability of GFP-  
316 TRAP affinity reagents, several groups have taken advantage of the fluorescent  
317 properties of GFP to confirm the correct localization of GFP tagged proteins, prior to  
318 purification and mass spectrometry analysis<sup>47</sup>. The main advantage of nanobody  
319 purification for protein complexes is the extremely low size of this molecule (~10kDa)

320 resulting in limited contamination of peptides generated from nanobodies after trypsin  
1 digestion, rendering mass spectrometry analysis of the purified protein complex more  
2 321 efficient<sup>48</sup>. However, caveats to tagging proteins with a GFP tag include the possible  
3 322 mislocalization of the fusion protein, hindering protein-protein interactions, and  
4 323 possible protein misfolding.  
5 324

### 325 **Purifying endogenous protein complexes using antibody immunoprecipitation**

326 The development of high affinity antibodies directed against proteins of interest  
17 327 allows the purification of large amounts of endogenous proteins and their associated  
18 328 partners amenable to mass spectrometry identification. The success of this method is  
19 329 highly dependent on the quality of the antibodies - in terms of affinity and specificity.  
20 330 The main advantage of this method is that the number of false positives is limited, as  
21 331 the targeted protein is not artificially overexpressed, and that it is localized in its  
22 332 natural subcellular compartment. This technique has been successful in describing  
23 333 the molecular components of the SCRIB complex and their role in cell migration<sup>49</sup>,  
24 334 and in characterizing the role of endogenous binding partners of VANGL2 and their  
25 335 functional importance in basal breast cancer progression<sup>50</sup>. One major drawback of  
26 336 this approach is that when the protein of interest is expressed at very low levels, the  
27 337 MS identification of co-purified proteins is difficult. These limitations are  
28 338 counterbalanced by the constant improvement in sensitivity of mass spectrometry  
29 339 devices and the development of high affinity antibodies.  
30  
31  
32

### 340 **Proteomics techniques defining the near neighborhood of a given protein of** 341 **interest**

342 With the recent development of new technologies based on proximal biotinylation  
58 343 and of highly sensitive MS devices, it is now possible to go a step further and explore  
59  
60  
61  
62  
63  
64  
65

1  
2  
3  
4  
5  
6  
7  
8  
9  
10  
11  
12  
13  
14  
15  
16  
17  
18  
19  
20  
21  
22  
23  
24  
25  
26  
27  
28  
29  
30  
31  
32  
33  
34  
35  
36  
37  
38  
39  
40  
41  
42  
43  
44  
45  
46  
47  
48  
49  
50  
51  
52  
53  
54  
55  
56  
57  
58  
59  
60  
61  
62  
63  
64  
65

344 larger protein complexes, and even to exhaustively characterize a specific cellular  
345 compartment. These methods take advantage of enzymes such as the biotin protein  
346 ligase BirA, the engineered ascorbate peroxidase (APEX), or the horseradish  
347 peroxidase HRP to promote the biotinylation of proteins in the immediate  
348 neighborhood of a protein of interest in living cells. Biotinylated proteins are  
349 subsequently isolated by affinity purification and identified by mass spectrometry  
350 analysis.

351 Over the last few years, several techniques have been developed. The first technique  
352 exploits the capacity of a bacterial biotin ligase (BirA) to covalently biotinylate  
353 proteins in living cells. A BirA mutant called proximity-dependent biotin identification  
354 (BioID) was designed and fused to proteins of interest for expression in cells<sup>51</sup>. BioID  
355 has a significantly lower affinity for biotinoyl-adenylate (bio-AMP), an intermediate of  
356 the biotinylation reaction, which is released from the binding pocket of BirA to the  
357 immediate neighborhood. Recently, a smaller form of BioID called BioID2<sup>52</sup> has been  
358 developed. This second generation enzyme is more efficient to label proteins with  
359 lower concentrations of biotin. Yet, one major drawback of this technique is the rate  
360 of the biotinylation reaction which can take up to 24 hours, rendering this technique  
361 unsuitable to decipher the transient activation of signaling pathways. Nevertheless,  
362 this approach has allowed the identification of molecular components of focal  
363 adhesions<sup>53</sup>. By probing several known components of the focal adhesion complex,  
364 Dong et al. were able to define different layers of neighborhood proteins (proximal to  
365 the membrane, intermediate layer, F-actin layer)<sup>53</sup>. The datasets obtained with this  
366 approach correlate closely with cellular imaging data using high resolution  
367 microscopy<sup>54</sup>. Other studies fused the biotin ligase to cell polarity components used  
368 as baits (E-cadherin<sup>55</sup>, ZO-1<sup>56</sup>, occludin and Claudin-4<sup>57</sup>) and expressed in

1  
2 370 polarized MDCK cells allowing the identification of known as well as novel protein  
3 networks<sup>55</sup>.

4  
5 371 Another recently developed biotinylation approach uses a modified peroxidase,  
6 ascorbate peroxidase (APEX) first developed for electromicroscopy studies<sup>58; 59</sup>. The  
7 labeling radius of biotinylation has been estimated to be less than 20nm and the half-  
8 372 life of the biotin-phenoxyl radical is shorter than that of bio-AMP rendering the labelling  
9 radius narrower. An optimized form of the APEX enzyme (APEX2) has recently been  
10 373 developed with greater enzymatic stability and activity<sup>60</sup>. As for BioID, the main  
11 advantage of this approach is that labelling of the proximal proteins occurs in living  
12 374 cells which decreases the rate of false positive as compared to other affinity  
13 purification-based strategies. Several studies have successfully used APEX  
14 375 biotinylation, notably to describe the protein composition of confined cellular  
15 compartments such as cilia<sup>61</sup> or mitochondria<sup>58; 62</sup>. In other studies, this approach  
16 376 was used to determine the spatiotemporal recruitment of proteins during the  
17 activation of signaling pathways such as the GPCR signaling<sup>63; 64</sup>.

18 377  
19 378  
20 379  
21 380  
22 381  
23 382  
24 383  
25 384 Optimization of the biotinylation protocol has been recently described using a  
26 common horseradish peroxidase (HRP) available in routine in laboratories. This  
27 385 method uses the properties of the HRP to proximally label proteins at the cell surface.  
28 In contrast to the APEX system, mature HRP needs to form disulfide bonds in order  
29 386 to be active, restricting its use to the extracellular environment<sup>65</sup>. HRP has a higher  
30 intrinsic peroxidase activity than APEX2 and can be used either with the membrane  
31 permeable biotin-phenol or with a membrane non-permeable version of the biotin-  
32 387 phenol called BxxP which harbors a polar polyamide linker. This approach allows the  
33 proteomics analysis of extracellular environments and it was recently employed to  
34 388 determine the composition of the proteome within the neuronal synaptic cleft<sup>65</sup>.

## 394 Proteomics approaches to analyze PAR functions

1  
2  
3 395 In 1983, work pioneered by Ken Kemphues and Jim Priess using a screen for  
4  
5 396 mutants defective in cell polarity in *C. elegans* identified the *par* genes . The mutants  
6  
7  
8 397 failed to form the endoderm because of defective partitioning of protein components  
9  
10 398 between anterior and posterior poles of the early embryos<sup>66; 67</sup>. PAR proteins, with  
11  
12  
13 399 the exception of PAR-2, are highly conserved in model organisms including *C.*  
14  
15 400 *elegans*, *Drosophila* and mammals <sup>68</sup>. PAR family proteins are involved in epithelial  
16  
17  
18 401 morphogenesis and contain two serine-threonine protein kinases, PAR-1 and PAR-4  
19  
20 402 (also known as STK11 or LKB1), a phospho- protein PAR-5 (a 14-3-3 isoform) and  
21  
22  
23 403 two scaffold proteins containing PDZ domains, PAR-3 and PAR-6. Atypical PKC  
24  
25 404 (aPKC) and CDC42 were demonstrated as crucial downstream polarity effector  
26  
27  
28 405 proteins in this pathway. In vertebrates, multiple copies of the *PAR* genes have been  
29  
30 406 identified, three for *PAR-6*, two for *PAR-3* and *aPKC*, and they are thought to have  
31  
32 407 different functions. Recently, only PAR-3L, and not PAR-3, has been shown to be  
33  
34  
35 408 involved in mammary gland stem cell maintenance through binding and suppression  
36  
37 409 of LKB1 kinase activity<sup>69</sup>. At the cellular level, PAR proteins are asymmetrically  
38  
39  
40 410 localized in polarized epithelial cells<sup>68</sup>. The apical domain is enriched in CDC42 and  
41  
42 411 PAR-6/aPKC, whereas cell-cell junctions are enriched in PAR-3 and PAR-1. During  
43  
44  
45 412 polarization, PAR-3 acts as a crucial landmark, which localizes at the apical portion of  
46  
47 413 cell-cell contacts, and then recruits other components of the adherens junctions.  
48  
49  
50 414 Therefore it acts as a transient docking site for PAR-6/aPKC and Crb/CDC42<sup>70; 43; 69</sup>  
51  
52 415 and allows apico-basal polarity to be established.

53  
54  
55 416 Mass spectrometry methods have been used to comprehensively analyze the human  
56  
57  
58 417 PAR protein complexes in 2004<sup>71</sup>, with the aim to determine whether the PAR  
59  
60 418 orthologues have common or different protein partners. TAP-tagged fusion proteins

1  
2  
3  
4  
5  
6  
7  
8  
9  
10  
11  
12  
13  
14  
15  
16  
17  
18  
19  
20  
21  
22  
23  
24  
25  
26  
27  
28  
29  
30  
31  
32  
33  
34  
35  
36  
37  
38  
39  
40  
41  
42  
43  
44  
45  
46  
47  
48  
49  
50  
51  
52  
53  
54  
55  
56  
57  
58  
59  
60  
61  
62  
63  
64  
65

419 of the PAR “core members”, including PAR-1, PAR-3, PAR-4, PAR-5, PAR-6A, PAR-  
420 6B, PAR-6C and PKC $\lambda$ <sup>39</sup> were independently expressed, resulting in the identification  
421 of a total of 60 proteins, which include partners directly or indirectly linked to cell  
422 polarity such as Hensin and mSpaghetti (also known as MLCK-like protein)<sup>72</sup>. More  
423 than 50 novel interactors were identified, some of which, such as the 14-3-3  
424 phospho-protein scaffolds, were present in more than one distinct complex<sup>71</sup>.

425 Furthermore, immunoprecipitation of FLAG-tagged PAR-3s, followed by mass  
426 spectrometry analysis, identified the serine-threonine protein phosphatase PP1  
427 (predominantly the alpha isoform) as a binding partner of PAR-3<sup>73</sup>. PAR-3 is  
428 phosphorylated by PAR-1 which leads to dissociation from aPKC and association  
429 with 14-3-3 and PAR-3 at the basolateral membrane<sup>74; 75</sup>. Dephosphorylation of PAR-  
430 3 by PP1 $\alpha$  frees 14-3-3, which in turn restores the association of PAR-3 with aPKC,  
431 and therefore the relocalization of a functional complex to tight junctions<sup>73</sup>. Mass  
432 spectrometry analysis allowed the identification of Serine 144 and Serine 885 of  
433 PAR-3 as residues that are dephosphorylated by PP1. This data confirmed  
434 previously published work, highlighting the critical role of PAR-3 phosphorylation.  
435 Accordingly, expression of a mutant of PAR-3 deficient in Serine 144 phosphorylation  
436 results in epithelial cell polarity defects<sup>75</sup>. Together these data provide a clear  
437 understanding of the molecular mechanism controlling PAR-3 localization and  
438 maintenance at the tight junctions of epithelial cells (FIGURE 3).

439 The LKB1 homologue, PAR-4, was originally ascribed a role in asymmetric cell  
440 division in *C. elegans*<sup>67</sup>. LKB1 is described as a “master” kinase of epithelial polarity  
441 establishment<sup>76</sup> through its association with the STRAD- $\alpha$  or - $\beta$  pseudo-kinases and  
442 the adaptor MO25. LKB1 is able to phosphorylate up to 14 downstream kinases,  
443 including AMPK or PAR-1, which in turn phosphorylate various downstream

444 components such as RAPTOR or PAR-3. LKB1 and its regulatory subunits STRAD  
1  
2 445 localize at the adherens junctions in an E-cadherin dependent manner<sup>77</sup>, controlling  
3  
4 446 local AMPK activation and MLC phosphorylation, which in turn leads to constriction of  
5  
6  
7 447 the apical cytoskeleton<sup>78</sup>. In mammals, *LKB1* acts as a tumor suppressor and is  
8  
9  
10 448 responsible for the Peutz-Jegher syndrome, an autosomal dominant inherited  
11  
12 449 disorder causing gastrointestinal hamartomatous polyposis and increased  
13  
14 450 predisposition to cancer in colon, breast, ovarian, pancreatic and lung tissues. *LKB1*  
15  
16  
17 451 is also somatically mutated in lung or cervical carcinoma and synergizes with human  
18  
19 452 papilloma viruses as its loss promotes disease progression<sup>79</sup>. Yeast two hybrid  
20  
21  
22 453 screens have allowed the first identification of the pseudo-kinases STRADs as  
23  
24 454 interacting partners of LKB1<sup>80</sup>. Upon binding to STRADs, LKB1 becomes active and  
25  
26  
27 455 autophosphorylates: mass spectrometry confirmed the existence of two previously  
28  
29 456 identified phosphorylation sites (Threonines 336 and 363) and detected two novel  
30  
31  
32 457 autophosphorylation sites on Threonines 185 and 402, which correlate with  
33  
34 458 increased LKB1 catalytic activity (FIGURE 3)<sup>80</sup>. A year later, an immunopurification  
35  
36  
37 459 procedure followed by mass spectrometry analysis led to the identification of LKB1-  
38  
39 460 associated proteins, including MO25, which stabilizes LKB1 in a LKB1-STRADs-  
40  
41 461 MO25 tripartite complex<sup>81</sup>. To further understand the molecular components  
42  
43  
44 462 associated with LKB1, two independent studies used mass spectrometry analysis of  
45  
46  
47 463 the purified LKB1 protein complex, and identified HSP90 as a chaperone protein  
48  
49 464 protecting LKB1 from proteasomal degradation<sup>82 83</sup>. In a later study, Hans Clevers's  
50  
51 465 team showed that the full activation of the kinase activity of LKB1 by STRADs results  
52  
53  
54 466 in the remodeling of the actin cytoskeleton, leading to the formation of an apical  
55  
56 467 brush border in isolated epithelial cells. These data suggest that LKB1 behaves as a  
57  
58 468 master regulator of apico-basal polarity in epithelial cells<sup>76</sup>. Although downstream  
59  
60  
61  
62  
63  
64  
65

1  
2  
3  
4  
5  
6  
7  
8  
9  
10  
11  
12  
13  
14  
15  
16  
17  
18  
19  
20  
21  
22  
23  
24  
25  
26  
27  
28  
29  
30  
31  
32  
33  
34  
35  
36  
37  
38  
39  
40  
41  
42  
43  
44  
45  
46  
47  
48  
49  
50  
51  
52  
53  
54  
55  
56  
57  
58  
59  
60  
61  
62  
63  
64  
65

469 signaling of LKB1 is well defined, the mechanisms of regulation and activation of this  
470 serine/threonine kinase remains elusive and deserve further investigation.

### 471 **Proteomics applied to study the Crumbs complex**

472 The second conserved polarity complex is the Crumbs complex. The *crumbs (crb)*  
473 gene, originally identified in *Drosophila*<sup>84</sup>, was first shown to be important in the  
474 establishment of epithelial polarity in 1990s<sup>85</sup>. Four proteins are considered to be the  
475 core components of the *Drosophila* Crumbs complex: CRB, Stardust (SDT), PATJ  
476 (protein associated with tight junctions or Pals1-associated tight junction protein) and  
477 Lin-7<sup>86</sup>. CRB is a type-I transmembrane protein containing two highly conserved  
478 regions in its 37-amino-acid cytoplasmic domain which are crucial for its polarity  
479 functions: the C-terminal PDZ-binding motif and the FERM-binding domain<sup>86</sup>. The  
480 PDZ-binding motif is responsible for its interaction with PAR-6 and its partner aPKC,  
481 as well as MAGUKs and SDT<sup>87; 88; 89; 90; 91; 92</sup>. The juxtamembrane Four-point-one,  
482 Ezrin, Radixin, Moesin (FERM)-binding motif (FBM) has been reported to bind the  
483 FERM domain proteins Yurt and Moesin (Moe)<sup>93; 94</sup>. CRB was shown to be linked to  
484 Hippo signaling as FLAG-tagged YAP and TAZ bind to Crumbs polarity partners  
485 identified by mass spectrometry analysis, including PALS1, PATJ (or INADL),  
486 MUPP1, LIN7C, and AMOT<sup>95</sup>. The WW-domain and PDZ-binding motifs of YAP/TAZ  
487 are required for binding to the multiple members of the Crumbs complex<sup>95</sup>. YAP/TAZ  
488 interaction with Crumbs is required to suppress TGF- $\beta$  signaling, and consequently  
489 important for TGF $\beta$ -mediated epithelial-to-mesenchymal transition<sup>95</sup>. At the molecular  
490 level, YAP/TAZ retains phospho-SMAD in the cytosol, thus suppressing TGF- $\beta$   
491 signaling. In *Drosophila*, the Crumbs complex is linked to the Hippo pathway by  
492 binding to the FERM protein, Expanded, leading to its recruitment at the apical  
493 membrane of the peripodial epithelium of imaginal discs<sup>96</sup>. Recently, a siRNA screen

1  
2  
3  
4  
5  
6  
7  
8  
9  
10  
11  
12  
13  
14  
15  
16  
17  
18  
19  
20  
21  
22  
23  
24  
25  
26  
27  
28  
29  
30  
31  
32  
33  
34  
35  
36  
37  
38  
39  
40  
41  
42  
43  
44  
45  
46  
47  
48  
49  
50  
51  
52  
53  
54  
55  
56  
57  
58  
59  
60  
61  
62  
63  
64  
65

494 identified RNF146 and Tankyrases (TNKS1 and TNKS2) as regulators of PALS1  
495 subcellular localization. A proteomics approach using the BioID methodology has  
496 contributed to revealing the underlying molecular mechanism whereby RNF146 and  
497 TNSK2 target AMOTL2 for ubiquitin-dependent degradation and therefore blocking  
498 the inhibition of AMOTL2 over PALS1, which then relocates apically and stabilizes  
499 the Crumbs complex<sup>97</sup>. This finding is consistent with a previously published study  
500 which used single-step purification followed by mass spectrometry, and determined  
501 that YAP is associated with AMOTL2 and promotes inhibition of Hippo signaling<sup>98</sup>.  
502 The link between the Crumbs complex and Hippo or TGF- $\beta$  signaling to maintain  
503 apico-basal polarity is well characterized, however a more in-depth understanding of  
504 the role of each member of the Crumbs complex is still needed.

505

### 506 **Dissecting the molecular components of the SCRIB complex**

507 Scribble was initially identified at the septate junctions of *Drosophila* epithelial cells  
508 where it controls the distribution of apical proteins such as Crumbs<sup>99</sup>. Scribble  
509 behaves as a tumour suppressor by regulating cell polarity and growth, together with  
510 Lgl and Dlg<sup>99</sup>. The Scribble complex comprising these three gene products acts by  
511 antagonizing the spread of the apical domain promoted by the PAR complex<sup>100</sup>.  
512 Conversely, aPKC, bound to PAR6 and CDC42, acts downstream of Crumbs and  
513 PALS1, and phosphorylates LGL. This event leads to the exclusion of the Scribble  
514 complex from the apical membrane and to its relocalization to the basolateral one.  
515 The Scribble complex has also been shown to play a role in *Drosophila* neuroblast  
516 cell size and mitotic spindle asymmetry<sup>101</sup>. Human Scribble (or SCRIB) is composed  
517 of 16 amino-terminal leucine rich repeat (LRRs) and 4 carboxy-terminal PDZ protein

1 domains, as is the case for *Drosophila* Scribble, and is involved in the regulation of  
2 cell adhesion, cell shape and cell polarity<sup>82</sup>. SCRIB was first identified through its  
3  
4 interaction with E6, an oncoprotein encoded by human papillomaviruse-16 (HPV-16).  
5  
6  
7 Infection of epithelial cells by HPV-16 results in lesions of cutaneous and mucosal  
8  
9  
10 epithelia, genital tissues and upper respiratory tracts. As E6 associates with an  
11  
12 ubiquitin ligase (E6AP) in infected cells, it promotes ubiquitination and proteosomal  
13  
14 degradation of its associated proteins. To identify E6 targets, a GST-E6AP has been  
15  
16  
17 used as bait and affinity-purified SCRIB was identified by mass spectrometry<sup>102</sup>.  
18  
19 Mechanistically, E6 harbors a PDZ-binding motif allowing its interaction with the PDZ  
20  
21  
22 domain-3 of SCRIB and its recruitment close to E6AP, which promotes SCRIB  
23  
24 degradation. Expression of E6 in epithelial cells results in reduced SCRIB levels (as  
25  
26  
27 well as the level of other PDZ proteins able to interact with the E6 PDZ-binding motif),  
28  
29 subsequently altering the integrity of cell-cell junctions<sup>103</sup>. The first attempt to identify  
30  
31  
32 the proteins endogenously associated to SCRIB was performed using  
33  
34 immunoprecipitation of proteins extracted from non-transformed mammary epithelial  
35  
36  
37 MCF10A cells followed by mass spectrometry. SCRIB was very efficiently co-purified  
38  
39  
40 with ARGHEF7, also known as  $\beta$ -PIX, a RhoGEF which directly interacts with the first  
41  
42  
43 and third SCRIB PDZ domains through its PDZ binding motif<sup>49; 104</sup>. The SCRIB/ $\beta$ -PIX  
44  
45  
46 complex is associated with the serine-threonine kinase PAK, and it was shown to be  
47  
48  
49 essential for cell survival when localized within the adherens junctions<sup>105</sup>. In neuronal  
50  
51  
52 cells, SCRIB anchors ARGHEF7/ $\beta$ -PIX at the plasma membrane, controlling calcium  
53  
54  
55 dependent exocytosis<sup>49</sup>. SCRIB also interacts via its PDZ domains with the C-  
56  
57  
58 terminal of Thyrotropin Stimulating Hormone Receptor, a GPCR, and controls its  
59  
60  
61 trafficking to the plasma membrane via the ARGHEF7/ $\beta$ -PIX-GIT-ARF6 pathway<sup>106</sup>.  
62  
63  
64  
65 Other studies have shown that SCRIB localizes adenomatous polyposis coli (APC) at

543 the adherens junctions and regulates cell cycle<sup>107</sup>, and the phosphatase PHLPP1 at  
1  
2 544 the plasma membrane, which negatively regulates AKT signaling<sup>108</sup>. SCRIB is a  
3  
4  
5 545 potent inhibitor of other signaling pathways in polarized epithelial cells (FIGURE 4).  
6  
7 546 For example, SCRIB recruits members of the Hippo pathway to adherens junctions  
8  
9  
10 547 and targets TAZ for degradation through ubiquitination by  $\beta$ -TRCP<sup>109</sup>. A single step  
11  
12 548 purification of SCRIB followed by mass spectrometry showed its interaction with  
13  
14 549 SHOC2 and M-RAS and its inhibitory role on ERK activation<sup>110</sup>. Conversely, in  
15  
16  
17 550 migrating astrocytes, SCRIB promotes CDC42 activity at the leading edge and  
18  
19 551 controls Golgi apparatus orientation and directed cell migration<sup>111</sup>. SCRIB is also  
20  
21  
22 552 involved in the orientation of lamellipodia and directs cell migration of endothelial  
23  
24 553 cells through the control of the RAB7-dependent endocytic machinery responsible for  
25  
26  
27 554  $\alpha$ 5-integrin internalization and degradation<sup>112</sup>. We have also shown that the SCRIB/ $\beta$ -  
28  
29 555 PIX complex controls PAK subcellular localization at the leading edge of breast  
30  
31  
32 556 cancer cells to promote cell migration<sup>113</sup>. More recently, a report has demonstrated  
33  
34 557 that the subtle subcellular localization of SCRIB at the plasma membrane is required  
35  
36 558 for its activity in animals<sup>114</sup>. Indeed, transgenic mice overexpressing a mutant form of  
37  
38  
39 559 SCRIB (mutation P305L within LRR13) previously shown to be unable to reach the  
40  
41 560 plasma membrane<sup>115; 116</sup> display multifocal hyperplasia of mammary glands and  
42  
43  
44 561 develop mammary tumors following the mislocalization of PTEN in the cytosol and  
45  
46 562 activation of the AKT/mTOR/S6K signaling pathway<sup>117</sup>. In other mouse models, as is  
47  
48  
49 563 the case in *Drosophila*<sup>118</sup>, downregulation of SCRIB synergizes with oncogenes (Myc  
50  
51 564 or Ras) in the promotion of tumorigenic transformation of epithelial cells<sup>119; 120</sup>.  
52  
53 565 However, the analysis of public datasets shows that SCRIB overexpression is also  
54  
55  
56 566 correlated with an increased risk of patient relapse<sup>108</sup>. Indeed, SCRIB can also  
57  
58 567 behave as an oncogenic protein in certain circumstances<sup>121</sup>. Since its first  
59  
60  
61  
62  
63  
64  
65

1  
2  
3  
4  
5  
6  
7  
8  
9  
10  
11  
12  
13  
14  
15  
16  
17  
18  
19  
20  
21  
22  
23  
24  
25  
26  
27  
28  
29  
30  
31  
32  
33  
34  
35  
36  
37  
38  
39  
40  
41  
42  
43  
44  
45  
46  
47  
48  
49  
50  
51  
52  
53  
54  
55  
56  
57  
58  
59  
60  
61  
62  
63  
64  
65

568 identification in 2000<sup>99</sup>, several attempts have been made to identify the SCRIB-  
569 associated protein network. Yeast two-hybrid screens have mostly resulted in the  
570 identification of direct interactors of the SCRIB PDZ domains<sup>103; 106; 111</sup>. The TAP-tag  
571 approach identified protein complexes associated with SCRIB and showed that it  
572 forms a ternary complex with a member of the PCP pathway (VANGL1) and  
573 NOS1AP distinctly from the ARGHEF7/ $\beta$ -PIX-GIT-PAK complex previously  
574 characterized by our group<sup>49</sup>. Clinical data showed that, in breast cancer, increased  
575 expression of VANGL1 and SCRIB is correlated with poor patient prognosis,  
576 suggesting that SCRIB may have protumoral functions. Accordingly, targeting  
577 VANGL1, NOS1AP or SCRIB expression by siRNAs decreased breast cancer cell  
578 migration<sup>108</sup>. In summary, several methods, including endogenous IP, TAP-tag or  
579 single-step purification methods, have been used to decipher the network of proteins  
580 associated to SCRIB in different cellular models, yielding similar and conflicting  
581 results<sup>49; 108; 110</sup> (FIGURE 5). Recently, two independent groups used proteomics to  
582 define the composition of the multi-molecular structures that connect integrins and  
583 the actin cytoskeleton in focal adhesions. The first group, led by Ed Manser, used a  
584 BioID strategy using as baits PAXILLIN, a cytoplasmic focal adhesion protein, and  
585 KIDLIN2 which directly binds to  $\beta$ 1-integrin. Mass spectrometry analysis of purified  
586 proteins reveals the molecular composition of focal adhesions and identified several  
587 previously uncharacterized proteins<sup>53</sup>. The second group, led by Martin Humphries,  
588 assembled and compared all available datasets generated by multiple mass  
589 spectrometry-based proteomics reports<sup>117; 122; 123; 124; 125</sup> in order to identify the  
590 composition of the multi-molecular structures linking integrins to the actin  
591 cytoskeleton. In both studies, several known SCRIB interactors, including  
592 ARGHEF7/ $\beta$ -PIX and GIT1, previously known to participate with SCRIB in cell

1  
2  
3  
4  
5  
6  
7  
8  
9  
10  
11  
12  
13  
14  
15  
16  
17  
18  
19  
20  
21  
22  
23  
24  
25  
26  
27  
28  
29  
30  
31  
32  
33  
34  
35  
36  
37  
38  
39  
40  
41  
42  
43  
44  
45  
46  
47  
48  
49  
50  
51  
52  
53  
54  
55  
56  
57  
58  
59  
60  
61  
62  
63  
64  
65

593 motility, have been identified<sup>53 38; 113</sup>. However, SCRIB was absent from the list of  
594 focal adhesion proteins, confirming our previous data obtained by  
595 immunofluorescence and confocal analysis<sup>113</sup> raising the important issue of the  
596 spatio-temporal association between SCRIB and the GIT-ARGHEF7/ $\beta$ -PIX during  
597 cell migration.

### 599 **Mass spectrometry-based determination of planar cell polarity networks**

600 Since the first description of PCP in 1982<sup>126</sup>, most studies have used a combination  
601 of genetic approaches to determine the organization of the PCP pathway and only a  
602 few have attempted to do this at the proteomics level. Here, we will mostly focus on  
603 two components of PCP signaling which we recently investigated using proteomics:  
604 the cytoplasmic PRICKLE1<sup>44; 127 128</sup> and the four transmembrane protein VANGL2<sup>38;</sup>  
605 <sup>50</sup>. These core PCP components have been also recently involved in cancer, where  
606 their high expression correlates with poor prognosis<sup>13</sup>. In order to understand their  
607 involvement in cancer, we and others have used proteomics to identify partners  
608 regulating their functions. Single-step purification of Flag-tagged forms of PRICKLE  
609 followed by mass spectrometry has identified several previously unknown interactors  
610 of PRICKLE1 and 2<sup>44</sup>. One of them was the serine-threonine kinase, MINK1. MINK1  
611 was previously shown to be required for PCP signaling in *Drosophila*<sup>129</sup> and to  
612 regulate convergent-extension in *Xenopus*<sup>130</sup>. However, the underlying mechanism  
613 of action was not known. We showed that PRICKLE1 is phosphorylated by MINK1,  
614 which leads to its relocalization to the plasma membrane via the endocytic pathway  
615 and contributes to its asymmetrical distribution during convergent-extension in  
616 *Xenopus* and PCP signaling in *Drosophila* ommatidia<sup>44</sup>. Mass spectrometry analysis

617 of PRICKLE1 also identified the MINK1 phosphorylation site which was functionally  
1  
2 618 characterized. Indeed, expression of a PRICKLE1 mutant unable to be  
3  
4 619 phosphorylated by MINK1 phenocopied PRICKLE1 loss in *Xenopus*<sup>44</sup>. The  
5  
6  
7 620 PRICKLE-MINK1 interaction is evolutionary conserved and, in breast cancer cells,  
8  
9 621 promotes cancer cell migration<sup>131</sup>. In addition to its binding to MINK1, PRICKLE1 also  
10  
11 622 interacts with ARGHAP21/24<sup>128</sup>, mTORC2<sup>127</sup>, and PHLDB2<sup>132</sup> which contribute to  
12  
13  
14 623 basal breast and gastric cancer cell dissemination (FIGURE 6). At the signaling level,  
15  
16  
17 624 PRICKLE1 controls the spatio-temporal activation of downstream events by inhibiting  
18  
19 625 Rho signaling and restricting Rac1 activation at the edge of cancer cells<sup>128</sup>. It also  
20  
21  
22 626 contributes to local activation of AKT and promotes remodeling of the actin  
23  
24 627 cytoskeleton<sup>127</sup>. Finally, through its interaction with PHLDB2, it regulates CLASP2  
25  
26  
27 628 localization at the plus-end of microtubules to promote focal adhesion turnover and  
28  
29 629  $\beta$ 1-integrin internalization<sup>127 132</sup>. Together these data demonstrate the importance of  
30  
31  
32 630 PRICKLE1 as a molecular platform able to spatially control downstream signaling  
33  
34 631 cascades<sup>133; 134</sup>. Other components of PCP signaling have also been studied by  
35  
36  
37 632 proteomics. SCRIB, a known interactor of VANGL1 and VANGL2, was genetically  
38  
39 633 characterized for its involvement in the PCP pathway during mouse embryonic  
40  
41 634 development<sup>135</sup>. As seen before, the SCRIB interactome was extensively and mostly  
42  
43  
44 635 characterized in epithelial and breast cancer cells<sup>38; 49; 108; 110</sup>. Although SCRIB acts  
45  
46  
47 636 as regulator of apico-basal polarity and PCP, little is known about the subset of  
48  
49 637 SCRIB partners involved in the two processes and their potential interactions. In the  
50  
51 638 study by Anastas et al., two distinct SCRIB complexes (VANGL/SCRIB/NOS1AP and  
52  
53 639 SCRIB/ARGHEF7/GIT/PAK) were found to control cell motility<sup>108; 111; 112; 113; 136</sup> and  
54  
55  
56 640 cancer progression<sup>108</sup> (FIGURE 6). More recently, attempts have been made to  
57  
58 641 identify and characterize the interactome of VANGL2. Genetic studies showed that

1  
2  
3  
4  
5  
6  
7  
8  
9  
10  
11  
12  
13  
14  
15  
16  
17  
18  
19  
20  
21  
22  
23  
24  
25  
26  
27  
28  
29  
30  
31  
32  
33  
34  
35  
36  
37  
38  
39  
40  
41  
42  
43  
44  
45  
46  
47  
48  
49  
50  
51  
52  
53  
54  
55  
56  
57  
58  
59  
60  
61  
62  
63  
64  
65

642 Vangl/Strabismus interacts with Prickle in *Drosophila*<sup>137; 138</sup> and *Xenopus*<sup>139</sup>. We used  
643 yeast-two hybrid to identify proteins bound to the mammalian VANGL2 PDZ binding  
644 sequence<sup>38</sup>. Among the positive clones, we identified SCRIB and SNX27. SNX27 is  
645 known to control the retrograde route of GPCR trafficking at the plasma membrane<sup>140</sup>  
646 and we found that, indeed, it is responsible for plasma membrane localization of  
647 VANGL2<sup>38</sup>. Thanks to the generation of a high affinity and specific antibody targeting  
648 VANGL2<sup>141</sup>, we were able to immunoprecipitate endogenous VANGL2 from breast  
649 cancer cells at levels amenable to MS identification. This led to the first identification  
650 of the endogenous interaction between VANGL2 and VANGL1, which requires the  
651 four transmembrane domains of these partners. Surprisingly, no PDZ proteins were  
652 found in the VANGL2 complex, which might be due to the IP procedure and/or to the  
653 low affinity of PDZ interactions. Instead, we identified a novel VANGL2 interactor,  
654 p62/SQSTM1 (Sequestosome-1) which acts synergistically with VANGL2 in  
655 regulating convergent-extension in *Xenopus*<sup>50</sup>. p62/SQSTM1 was shown to bind  
656 directly to the VANGL2 C-terminal region independently from the PDZ-binding  
657 sequence. *VANGL2* and *p62/SQSTM1* genes are upregulated in basal breast cancer  
658 and are markers of poor prognosis. The specific interaction between VANGL2 and  
659 p62/SQSTM1 occurs in endocytic vesicles of breast cancer cells and results in the  
660 recruitment of JNK, leading to its activation and to JNK-dependent cell proliferation<sup>50</sup>  
661 (FIGURE 6). PTK7 is a PCP tyrosine kinase receptor functionally linked to VANGL2  
662 in the mouse<sup>142; 143</sup>. However, no interaction has so far been observed between the  
663 two receptors. Using a myc-tagged version of PTK7 expressed into the animal pole of  
664 *Xenopus* embryos, the Borchers lab was able to identify by mass spectrometry  
665 RACK1 (receptor of activated protein kinase C 1) as a cytosolic binding partner of  
666 PTK7. RACK1 is involved in the membrane localization of Dishevelled, a PDZ protein

1  
2  
3  
4  
5  
6  
7  
8  
9  
10  
11  
12  
13  
14  
15  
16  
17  
18  
19  
20  
21  
22  
23  
24  
25  
26  
27  
28  
29  
30  
31  
32  
33  
34  
35  
36  
37  
38  
39  
40  
41  
42  
43  
44  
45  
46  
47  
48  
49  
50  
51  
52  
53  
54  
55  
56  
57  
58  
59  
60  
61  
62  
63  
64  
65

667 involved in PCP <sup>144</sup>. The authors subsequently showed that RACK1, like PTK7, is  
668 required for *Xenopus* neural tube closure. Interestingly, RACK1 also directly interacts  
669 with VANGL2 in *Zebrafish* and regulates PCP-related functions by localizing VANGL2  
670 at the plasma membrane <sup>145</sup>. Much work is still needed to clarify the organization and  
671 regulation of protein networks associated with the numerous PCP components.

### 672 673 **Proteomics of the primary cilia**

674 Primary cilia are non-motile microtubule-based structures that are protruding from the  
675 cell body of almost all vertebrate cells. They develop from the mother centriole of the  
676 centrosome and have an antenna-like organization at the apical membrane of  
677 polarized epithelial cells (FIGURE 3). These structures concentrate membrane  
678 receptors able to respond to diverse stimuli including soluble ligands, mechanical and  
679 thermal stress, and act as sensors to fluid flow <sup>146</sup>. Identification of protein  
680 components of primary cilia is important to understand their organization, signal  
681 transduction properties and their involvement in diseases called ciliopathies. Over the  
682 past 10 years, several groups have attempted to identify ciliary proteins by using a  
683 combined procedure of primary cilia isolation through successive steps of sucrose  
684 gradient centrifugation and detergent solubilization, followed by mass spectrometry  
685 analysis. This strategy led to the identification of ~200 putative cilia-related proteins  
686 in human bronchial epithelial cells <sup>147</sup>, then of more than 2,000 proteins in rod and  
687 cone photoreceptor sensory cilia <sup>148</sup>. The mouse kidney collecting duct cell line  
688 (IMCD3) which behaves as a polarized epithelial cell was also used as a model  
689 system to identify more than 2,900 ciliary proteins. However, known non-ciliary  
690 proteins were also identified in this study, questioning the specificity of the  
691 experimental procedure. Nevertheless, using a subtractive procedure combined with

692 protein correlation profiling, the authors were able to generate a refined list of 195  
1  
2 693 confirmed primary cilia proteins<sup>149</sup>. Another study based on protein correlation  
3  
4 694 profiling coupled to a semi-quantitative technique based mass spectrometry (SILAC :  
5  
6  
7 695 stable isotope labelling by amino acids in cell culture) identified SCRIB in  
8  
9 696 centrosomes<sup>150</sup>, which confirmed previous findings<sup>111</sup>. However, SCRIB has not been  
10  
11 697 identified as a cilia resident protein so far. Interestingly, VANGL2, a partner of  
12  
13 698 SCRIB, plays a role in the localization and orientation of primary cilia, and directional  
14  
15 699 fluid flow involved in embryonic development<sup>151</sup>. In the mouse, VANGL2 interacts  
16  
17 700 with the Bbs8 and Ift20 ciliary proteins in a complex required for PCP signaling in the  
18  
19 701 cochlea<sup>152</sup>. TAP-tag strategy has been used to identify interactions between  
20  
21 702 intraflagellar transport proteins and endocytic components in cilia in *zebrafish*<sup>153</sup>. The  
22  
23 703 group of M. Nachury used a TAP-tag strategy to connect Arf-like GTPases to cargo  
24  
25 704 entry into primary cilia<sup>154</sup>. More recently the same group used the APEX technique to  
26  
27 705 characterize the proteins composition of primary cilia using a domain of NPHP3 as  
28  
29 706 bait, which specifically localized in cilia. This approach generated a list of 622  
30  
31 707 putative ciliary proteins, including LKB1 and its partner STRAD $\beta$ <sup>61</sup>..  
32  
33  
34  
35  
36  
37  
38  
39  
40

## 709 **Future directions**

710 The rapidly increasing number of studies using mass spectrometry has resulted in  
711 the discovery of protein complexes associated with major polarity proteins and has  
712 been instrumental in deciphering some of their functions, which is expected to further  
713 continue thanks to novel protein purification methods such as proximity biotinylation  
714 (BioID, APEX) and access to more sensitive mass spectrometers. One of the best  
715 characterized polarity complexes which is centered on SCRIB has benefited from a  
716 combination of several purification and mass spectrometry improvements over the

1  
2  
3  
4  
5  
6  
7  
8  
9  
10  
11  
12  
13  
14  
15  
16  
17  
18  
19  
20  
21  
22  
23  
24  
25  
26  
27  
28  
29  
30  
31  
32  
33  
34  
35  
36  
37  
38  
39  
40  
41  
42  
43  
44  
45  
46  
47  
48  
49  
50  
51  
52  
53  
54  
55  
56  
57  
58  
59  
60  
61  
62  
63  
64  
65

717 last 15 years, leading to a comprehensive picture of the network at the steady state  
718 (FIGURE 5)<sup>49; 108; 110</sup>. However, there is currently no information about the  
719 composition, compartmentalization and spatio-temporal regulation of this protein  
720 complex during the different steps of epithelial morphogenesis and transformation.  
721 This issue is, in our opinion, of particular importance considering the multiple cellular  
722 localizations (adherens junctions, leading edge, centrosomes) of SCRIB and their  
723 now well established functional importance. This also applies to other cell polarity  
724 proteins (PAR, LKB1,...) in normal and pathological situations. We believe that the  
725 combination of proximity biotinylation techniques with CRISPR/Cas9 gene editing  
726 and proximity ligation assay (PLA)<sup>155</sup> may be key in deciphering and validating the  
727 composition of cell polarity interactomes in cells or tissues. PLA is an oligonucleotide-  
728 conjugated antibodies-based technique of particular interest to confirm low affinity  
729 direct interactions (for example PDZ interactions) which are not amenable to regular  
730 co-immunoprecipitations. Furthermore, PLA is suitable for the exploration of direct  
731 protein-protein interactions in tissues<sup>156</sup>.

732 Recently, Norbert Perrimon's group used APEX labeling in live *Drosophila* tissues to  
733 map the sub-proteomes of mitochondria in different physiological conditions<sup>62</sup>. This  
734 study demonstrates the feasibility of identifying proteomes (and surely, in the future,  
735 protein networks) *in vivo* in a more comprehensive manner than other procedures  
736 relying on TAP-tag techniques<sup>157</sup>.

737 Recent improvements of proximity biotinylation techniques may also help to assess  
738 the organization of polarity complexes, especially at the plasma membrane. A  
739 derivative of the APEX strategy based on the more sensitive HRP was recently  
740 developed to identify protein complexes present in the neuronal synaptic cleft<sup>65</sup>. By  
741 taking advantage of the inactivity of HRP in reducing intracellular compartments, it is

742 possible to specifically biotinylate proteins in secretory and extracellular  
1  
2 743 compartments. Furthermore, the use of a biotin-phenol derived substrate unable to  
3  
4  
5 744 cross the plasma membrane will specifically target the extracellular domains of  
6  
7 745 membrane proteins. This approach should be able to address yet answered issues  
8  
9  
10 746 such as the organization of membrane cell polarity receptors and co-receptors upon  
11  
12 747 ligand stimulation in different physiological and pathological situations <sup>13</sup>. A recent  
13  
14 748 alternative to this method relies on high affinity HRP-coupled antibodies, avoiding the  
15  
16  
17 749 need to ectopically express HRP-fused proteins in cells, and allowing the direct  
18  
19 750 identification of endogenous protein complexes including in fixed patient tissues  
20  
21  
22 751 samples <sup>158</sup>.

23  
24  
25 752 Two independent groups have recently optimized the APEX technology using anti-  
26  
27 753 biotin antibodies instead of streptavidin to purify trypsin-digested biotinylated proteins  
28  
29  
30 754 and have shown that this variant technique provides additional information,  
31  
32 755 quantitatively and qualitatively (spatial and topological organization of protein  
33  
34  
35 756 complexes) compared to the original method. <sup>159; 160</sup>.

36  
37  
38 757 Mass spectrometry can also provide important information about post-translational  
39  
40  
41 758 modifications the identification and function of which are poorly understood in cell  
42  
43 759 polarity complexes, with a few exceptions<sup>44; 73; 161; 162</sup>,. Notably, it has recently been  
44  
45 760 published that ciliary proteins contained high levels of non-canonical  
46  
47  
48 761 phosphopeptides of unknown function<sup>163</sup>. Obviously, many questions remain to be  
49  
50 762 answered before obtaining a comprehensive picture of the cell polarity processes but  
51  
52  
53 763 the development of novel sensitive mass spectrometry techniques should allow us  
54  
55 764 tackle this exciting challenge.

56  
57  
58 765

## 60 766 **Acknowledgments**

767 The authors thank Eric Bailly and Valerie Depraetere for critical review of the  
1  
2 768 manuscript. J-P.B.'s laboratory is funded by La Ligue Nationale Contre le Cancer  
3  
4 769 (Label Ligue J.P.B.), Institut National du Cancer (PLBIO INCa), Fondation ARC pour  
5  
6  
7 770 la Recherche sur le Cancer, Ruban Rose, A\*MIDEX: ANR-11-IDEX-0001-02, (T.P.)  
8  
9  
10 771 and SIRIC (INCa-DGOS-Inserm 6038, fellowship to A.M.D.). J-P.B. is a scholar of  
11  
12 772 Institut Universitaire de France.

13  
14 773

## 17 774 **References**

- 20 775 1. Margolis, B. & Borg, J. P. (2005). Apicobasal polarity complexes. *J Cell Sci* **118**, 5157-9.
- 21 776 2. Suzuki, A., Yamanaka, T., Hirose, T., Manabe, N., Mizuno, K., Shimizu, M., Akimoto, K., Izumi,  
22 777 Y., Ohnishi, T. & Ohno, S. (2001). Atypical protein kinase C is involved in the evolutionarily  
23 778 conserved par protein complex and plays a critical role in establishing epithelia-specific  
24 779 junctional structures. *J Cell Biol* **152**, 1183-96.
- 26 780 3. Bilder, D. (2004). Epithelial polarity and proliferation control: links from the Drosophila  
27 781 neoplastic tumor suppressors. *Genes Dev* **18**, 1909-25.
- 28 782 4. Khursheed, M. & Bashyam, M. D. (2014). Apico-basal polarity complex and cancer. *J Biosci*  
29 783 **39**, 145-55.
- 31 784 5. Bilder, D. & Perrimon, N. (2000). Localization of apical epithelial determinants by the  
32 785 basolateral PDZ protein Scribble. *Nature* **403**, 676-80.
- 33 786 6. Pocha, S. M. & Knust, E. (2013). Complexities of Crumbs function and regulation in tissue  
34 787 morphogenesis. *Curr Biol* **23**, R289-93.
- 36 788 7. Plant, P. J., Fawcett, J. P., Lin, D. C., Holdorf, A. D., Binns, K., Kulkarni, S. & Pawson, T. (2003).  
37 789 A polarity complex of mPar-6 and atypical PKC binds, phosphorylates and regulates  
38 790 mammalian Lgl. *Nat Cell Biol* **5**, 301-8.
- 39 791 8. Yamanaka, T., Horikoshi, Y., Sugiyama, Y., Ishiyama, C., Suzuki, A., Hirose, T., Iwamatsu, A.,  
40 792 Shinohara, A. & Ohno, S. (2003). Mammalian Lgl forms a protein complex with PAR-6 and  
41 793 aPKC independently of PAR-3 to regulate epithelial cell polarity. *Curr Biol* **13**, 734-43.
- 43 794 9. Zallen, J. A. (2007). Planar polarity and tissue morphogenesis. *Cell* **129**, 1051-63.
- 44 795 10. Tada, M. & Heisenberg, C. P. (2012). Convergent extension: using collective cell migration  
45 796 and cell intercalation to shape embryos. *Development* **139**, 3897-904.
- 46 797 11. Gao, B. (2012). Wnt regulation of planar cell polarity (PCP). *Curr Top Dev Biol* **101**, 263-95.
- 47 798 12. Harris, P. C. & Torres, V. E. (2009). Polycystic kidney disease. *Annu Rev Med* **60**, 321-37.
- 48 799 13. Daulat, A. M. & Borg, J. P. (2017). Wnt/Planar Cell Polarity Signaling: New Opportunities for  
49 800 Cancer Treatment. *Trends Cancer* **3**, 113-125.
- 51 801 14. Fraser, C. M., Gocayne, J. D., White, O., Adams, M. D., Clayton, R. A., Fleischmann, R. D., Bult,  
52 802 C. J., Kerlavage, A. R., Sutton, G., Kelley, J. M., Fritchman, R. D., Weidman, J. F., Small, K. V.,  
53 803 Sandusky, M., Fuhrmann, J., Nguyen, D., Utterback, T. R., Saudek, D. M., Phillips, C. A.,  
54 804 Merrick, J. M., Tomb, J. F., Dougherty, B. A., Bott, K. F., Hu, P. C., Lucier, T. S., Peterson, S. N.,  
55 805 Smith, H. O., Hutchison, C. A., 3rd & Venter, J. C. (1995). The minimal gene complement of  
56 806 *Mycoplasma genitalium*. *Science* **270**, 397-403.
- 58 807 15. Swinbanks, D. (1995). Government backs proteome proposal. *Nature* **378**, 653.

- 808 16. Smith, L. M. & Kelleher, N. L. (2013). Proteoform: a single term describing protein complexity. *Nat Methods* **10**, 186-7.
- 1 809
- 2 810 17. Blackstock, W. P. & Weir, M. P. (1999). Proteomics: quantitative and physical mapping of
- 3 811 cellular proteins. *Trends Biotechnol* **17**, 121-7.
- 4 812 18. Harper, J. W. & Bennett, E. J. (2016). Proteome complexity and the forces that drive
- 5 813 proteome imbalance. *Nature* **537**, 328-38.
- 6 814 19. Wilm, M. & Mann, M. (1996). Analytical properties of the nanoelectrospray ion source. *Anal*
- 7 815 *Chem* **68**, 1-8.
- 8 816 20. Nolting, D., Malek, R. & Makarov, A. (2017). Ion traps in modern mass spectrometry. *Mass*
- 9 817 *Spectrom Rev*.
- 10 818 21. Zhang, Y., Fonslow, B. R., Shan, B., Baek, M. C. & Yates, J. R., 3rd. (2013). Protein analysis by
- 11 819 shotgun/bottom-up proteomics. *Chem Rev* **113**, 2343-94.
- 12 820 22. Cox, J. & Mann, M. (2008). MaxQuant enables high peptide identification rates,
- 13 821 individualized p.p.b.-range mass accuracies and proteome-wide protein quantification. *Nat*
- 14 822 *Biotechnol* **26**, 1367-72.
- 15 823 23. Paulo, J. A. (2013). Practical and Efficient Searching in Proteomics: A Cross Engine
- 16 824 Comparison. *Webmedcentral* **4**.
- 17 825 24. Tyanova, S., Temu, T., Sinitcyn, P., Carlson, A., Hein, M. Y., Geiger, T., Mann, M. & Cox, J.
- 18 826 (2016). The Perseus computational platform for comprehensive analysis of (prote)omics
- 19 827 data. *Nat Methods* **13**, 731-40.
- 20 828 25. Vidova, V. & Spacil, Z. (2017). A review on mass spectrometry-based quantitative proteomics:
- 21 829 Targeted and data independent acquisition. *Anal Chim Acta* **964**, 7-23.
- 22 830 26. MacLean, B., Tomazela, D. M., Shulman, N., Chambers, M., Finney, G. L., Frewen, B., Kern, R.,
- 23 831 Tabb, D. L., Liebler, D. C. & MacCoss, M. J. (2010). Skyline: an open source document editor
- 24 832 for creating and analyzing targeted proteomics experiments. *Bioinformatics* **26**, 966-8.
- 25 833 27. Hu, A., Noble, W. S. & Wolf-Yadlin, A. (2016). Technical advances in proteomics: new
- 26 834 developments in data-independent acquisition. *F1000Res* **5**.
- 27 835 28. Bilbao, A., Varesio, E., Luban, J., Strambio-De-Castillia, C., Hopfgartner, G., Muller, M. &
- 28 836 Lisacek, F. (2015). Processing strategies and software solutions for data-independent
- 29 837 acquisition in mass spectrometry. *Proteomics* **15**, 964-80.
- 30 838 29. Rost, H. L., Rosenberger, G., Navarro, P., Gillet, L., Miladinovic, S. M., Schubert, O. T., Wolski,
- 31 839 W., Collins, B. C., Malmstrom, J., Malmstrom, L. & Aebersold, R. (2014). OpenSWATH enables
- 32 840 automated, targeted analysis of data-independent acquisition MS data. *Nat Biotechnol* **32**,
- 33 841 219-23.
- 34 842 30. Kelleher, N. L. (2004). Top-down proteomics. *Anal Chem* **76**, 197A-203A.
- 35 843 31. Taylor, G. K., Kim, Y. B., Forbes, A. J., Meng, F., McCarthy, R. & Kelleher, N. L. (2003). Web and
- 36 844 database software for identification of intact proteins using "top down" mass spectrometry.
- 37 845 *Anal Chem* **75**, 4081-6.
- 38 846 32. Cristobal, A., Marino, F., Post, H., van den Toorn, H. W., Mohammed, S. & Heck, A. J. (2017).
- 39 847 Toward an Optimized Workflow for Middle-Down Proteomics. *Anal Chem* **89**, 3318-3325.
- 40 848 33. Chahrour, O., Cobice, D. & Malone, J. (2015). Stable isotope labelling methods in mass
- 41 849 spectrometry-based quantitative proteomics. *J Pharm Biomed Anal* **113**, 2-20.
- 42 850 34. Gerber, S. A., Rush, J., Stemman, O., Kirschner, M. W. & Gygi, S. P. (2003). Absolute
- 43 851 quantification of proteins and phosphoproteins from cell lysates by tandem MS. *Proc Natl*
- 44 852 *Acad Sci U S A* **100**, 6940-5.
- 45 853 35. Becamel, C., Alonso, G., Galeotti, N., Demey, E., Jouin, P., Ullmer, C., Dumuis, A., Bockaert, J.
- 46 854 & Marin, P. (2002). Synaptic multiprotein complexes associated with 5-HT(2C) receptors: a
- 47 855 proteomic approach. *EMBO J* **21**, 2332-42.
- 48 856 36. Maurice, P., Daulat, A. M., Broussard, C., Mozo, J., Clary, G., Hotellier, F., Chafey, P.,
- 49 857 Guillaume, J. L., Ferry, G., Boutin, J. A., Delagrance, P., Camoin, L. & Jockers, R. (2008). A
- 50 858 generic approach for the purification of signaling complexes that specifically interact with the
- 51 859 carboxyl-terminal domain of G protein-coupled receptors. *Mol Cell Proteomics* **7**, 1556-69.
- 52 859
- 53
- 54
- 55
- 56
- 57
- 58
- 59
- 60
- 61
- 62
- 63
- 64
- 65

- 860 37. Daulat, A. M., Maurice, P., Froment, C., Guillaume, J. L., Broussard, C., Monsarrat, B.,  
1 861 Delagrangé, P. & Jockers, R. (2007). Purification and identification of G protein-coupled  
2 862 receptor protein complexes under native conditions. *Mol Cell Proteomics* **6**, 835-44.
- 3 863 38. Belotti, E., Polanowska, J., Daulat, A. M., Audebert, S., Thome, V., Lissitzky, J. C., Lembo, F.,  
4 864 Blibek, K., Omi, S., Lenfant, N., Gangar, A., Montcouquiol, M., Santoni, M. J., Sebbagh, M.,  
5 865 Aurrand-Lions, M., Angers, S., Kodjabachian, L., Reboul, J. & Borg, J. P. (2013). The human  
6 866 PDZome: a gateway to PSD95-Disc large-zonula occludens (PDZ)-mediated functions. *Mol Cell*  
7 867 *Proteomics* **12**, 2587-603.
- 8 868 39. Rigaut, G., Shevchenko, A., Rutz, B., Wilm, M., Mann, M. & Seraphin, B. (1999). A generic  
9 869 protein purification method for protein complex characterization and proteome exploration.  
10 870 *Nat Biotechnol* **17**, 1030-2.
- 11 871 40. Gavin, A. C., Bosche, M., Krause, R., Grandi, P., Marzioch, M., Bauer, A., Schultz, J., Rick, J. M.,  
12 872 Michon, A. M., Cruciat, C. M., Remor, M., Hofert, C., Schelder, M., Brajenovic, M., Ruffner, H.,  
13 873 Merino, A., Klein, K., Hudak, M., Dickson, D., Rudi, T., Gnau, V., Bauch, A., Bastuck, S., Huhse,  
14 874 B., Leutwein, C., Heurtier, M. A., Copley, R. R., Edelmann, A., Querfurth, E., Rybin, V., Drewes,  
15 875 G., Raida, M., Bouwmeester, T., Bork, P., Seraphin, B., Kuster, B., Neubauer, G. & Superti-  
16 876 Furga, G. (2002). Functional organization of the yeast proteome by systematic analysis of  
17 877 protein complexes. *Nature* **415**, 141-7.
- 18 878 41. Bouwmeester, T., Bauch, A., Ruffner, H., Angrand, P. O., Bergamini, G., Croughton, K., Cruciat,  
19 879 C., Eberhard, D., Gagneur, J., Ghidelli, S., Hopf, C., Huhse, B., Mangano, R., Michon, A. M.,  
20 880 Schirle, M., Schlegl, J., Schwab, M., Stein, M. A., Bauer, A., Casari, G., Drewes, G., Gavin, A. C.,  
21 881 Jackson, D. B., Joberty, G., Neubauer, G., Rick, J., Kuster, B. & Superti-Furga, G. (2004). A  
22 882 physical and functional map of the human TNF-alpha/NF-kappa B signal transduction  
23 883 pathway. *Nat Cell Biol* **6**, 97-105.
- 24 884 42. Angers, S., Thorpe, C. J., Biechele, T. L., Goldenberg, S. J., Zheng, N., MacCoss, M. J. & Moon,  
25 885 R. T. (2006). The KLHL12-Cullin-3 ubiquitin ligase negatively regulates the Wnt-beta-catenin  
26 886 pathway by targeting Dishevelled for degradation. *Nat Cell Biol* **8**, 348-57.
- 27 887 43. Lui, T. T., Lacroix, C., Ahmed, S. M., Goldenberg, S. J., Leach, C. A., Daulat, A. M. & Angers, S.  
28 888 (2011). The ubiquitin-specific protease USP34 regulates axin stability and Wnt/beta-catenin  
29 889 signaling. *Mol Cell Biol* **31**, 2053-65.
- 30 890 44. Daulat, A. M., Luu, O., Sing, A., Zhang, L., Wrana, J. L., McNeill, H., Winklbauer, R. & Angers, S.  
31 891 (2012). Mink1 regulates beta-catenin-independent Wnt signaling via Prickle phosphorylation.  
32 892 *Mol Cell Biol* **32**, 173-85.
- 33 893 45. Goudreault, M., D'Ambrosio, L. M., Kean, M. J., Mullin, M. J., Larsen, B. G., Sanchez, A.,  
34 894 Chaudhry, S., Chen, G. I., Sicheri, F., Nesvizhskii, A. I., Aebersold, R., Raught, B. & Gingras, A.  
35 895 C. (2009). A PP2A phosphatase high density interaction network identifies a novel striatin-  
36 896 interacting phosphatase and kinase complex linked to the cerebral cavernous malformation 3  
37 897 (CCM3) protein. *Mol Cell Proteomics* **8**, 157-71.
- 38 898 46. Mellacheruvu, D., Wright, Z., Couzens, A. L., Lambert, J. P., St-Denis, N. A., Li, T., Miteva, Y. V.,  
39 899 Hauri, S., Sardi, M. E., Low, T. Y., Halim, V. A., Bagshaw, R. D., Hubner, N. C., Al-Hakim, A.,  
40 900 Bouchard, A., Faubert, D., Fermin, D., Dunham, W. H., Goudreault, M., Lin, Z. Y., Badillo, B. G.,  
41 901 Pawson, T., Durocher, D., Coulombe, B., Aebersold, R., Superti-Furga, G., Colinge, J., Heck, A.  
42 902 J., Choi, H., Gstaiger, M., Mohammed, S., Cristea, I. M., Bennett, K. L., Washburn, M. P.,  
43 903 Raught, B., Ewing, R. M., Gingras, A. C. & Nesvizhskii, A. I. (2013). The CRAPome: a  
44 904 contaminant repository for affinity purification-mass spectrometry data. *Nat Methods* **10**,  
45 905 730-6.
- 46 906 47. Bouguenina, H., Salaun, D., Mangon, A., Muller, L., Baudelet, E., Camoin, L., Tachibana, T.,  
47 907 Cianferani, S., Audebert, S., Verdier-Pinard, P. & Badache, A. (2017). EB1-binding-myomegalin  
48 908 protein complex promotes centrosomal microtubules functions. *Proc Natl Acad Sci U S A* **114**,  
49 909 E10687-E10696.
- 50 910 48. Verdier-Pinard, P., Salaun, D., Bouguenina, H., Shimada, S., Pophillat, M., Audebert, S.,  
51 911 Agavnian, E., Coslet, S., Charafe-Jauffret, E., Tachibana, T. & Badache, A. (2017). Septin 9\_i2 is

- 912 downregulated in tumors, impairs cancer cell migration and alters subnuclear actin filaments.  
 1 913 *Sci Rep* **7**, 44976.
- 2 914 49. Audebert, S., Navarro, C., Nourry, C., Chasserot-Golaz, S., Lecine, P., Bellaiche, Y., Dupont, J.  
 3 915 L., Premont, R. T., Sempere, C., Strub, J. M., Van Dorsselaer, A., Vitale, N. & Borg, J. P. (2004).  
 4 916 Mammalian Scribble forms a tight complex with the betaPIX exchange factor. *Curr Biol* **14**,  
 5 917 987-95.
- 7 918 50. Puvirajesinghe, T. M., Bertucci, F., Jain, A., Scerbo, P., Belotti, E., Audebert, S., Sebbagh, M.,  
 8 919 Lopez, M., Brech, A., Finetti, P., Charafe-Jauffret, E., Chaffanet, M., Castellano, R., Restouin,  
 9 920 A., Marchetto, S., Collette, Y., Goncalves, A., Macara, I., Birnbaum, D., Kodjabachian, L.,  
 10 921 Johansen, T. & Borg, J. P. (2016). Identification of p62/SQSTM1 as a component of non-  
 11 922 canonical Wnt VANGL2-JNK signalling in breast cancer. *Nat Commun* **7**, 10318.
- 13 923 51. Roux, K. J., Kim, D. I., Raida, M. & Burke, B. (2012). A promiscuous biotin ligase fusion protein  
 14 924 identifies proximal and interacting proteins in mammalian cells. *J Cell Biol* **196**, 801-10.
- 15 925 52. Kim, D. I., Jensen, S. C., Noble, K. A., Kc, B., Roux, K. H., Motamedchaboki, K. & Roux, K. J.  
 16 926 (2016). An improved smaller biotin ligase for BiOD proximity labeling. *Mol Biol Cell* **27**, 1188-  
 17 927 96.
- 19 928 53. Dong, J. M., Tay, F. P., Swa, H. L., Gunaratne, J., Leung, T., Burke, B. & Manser, E. (2016).  
 20 929 Proximity biotinylation provides insight into the molecular composition of focal adhesions at  
 21 930 the nanometer scale. *Sci Signal* **9**, rs4.
- 22 931 54. Kanchanawong, P., Shtengel, G., Pasapera, A. M., Ramko, E. B., Davidson, M. W., Hess, H. F. &  
 23 932 Waterman, C. M. (2010). Nanoscale architecture of integrin-based cell adhesions. *Nature*  
 24 933 **468**, 580-4.
- 26 934 55. Van Itallie, C. M. & Anderson, J. M. (2014). Architecture of tight junctions and principles of  
 27 935 molecular composition. *Semin Cell Dev Biol* **36**, 157-65.
- 28 936 56. Van Itallie, C. M., Aponte, A., Tietgens, A. J., Gucek, M., Fredriksson, K. & Anderson, J. M.  
 29 937 (2013). The N and C termini of ZO-1 are surrounded by distinct proteins and functional  
 30 938 protein networks. *J Biol Chem* **288**, 13775-88.
- 32 939 57. Fredriksson, K., Van Itallie, C. M., Aponte, A., Gucek, M., Tietgens, A. J. & Anderson, J. M.  
 33 940 (2015). Proteomic analysis of proteins surrounding occludin and claudin-4 reveals their  
 34 941 proximity to signaling and trafficking networks. *PLoS One* **10**, e0117074.
- 35 942 58. Hung, V., Zou, P., Rhee, H. W., Udeshi, N. D., Cracan, V., Svinkina, T., Carr, S. A., Mootha, V. K.  
 36 943 & Ting, A. Y. (2014). Proteomic mapping of the human mitochondrial intermembrane space  
 37 944 in live cells via ratiometric APEX tagging. *Mol Cell* **55**, 332-41.
- 39 945 59. Rhee, H. W., Zou, P., Udeshi, N. D., Martell, J. D., Mootha, V. K., Carr, S. A. & Ting, A. Y.  
 40 946 (2013). Proteomic mapping of mitochondria in living cells via spatially restricted enzymatic  
 41 947 tagging. *Science* **339**, 1328-1331.
- 42 948 60. Lam, S. S., Martell, J. D., Kamer, K. J., Deerinck, T. J., Ellisman, M. H., Mootha, V. K. & Ting, A.  
 43 949 Y. (2015). Directed evolution of APEX2 for electron microscopy and proximity labeling. *Nat*  
 44 950 *Methods* **12**, 51-4.
- 46 951 61. Mick, D. U., Rodrigues, R. B., Leib, R. D., Adams, C. M., Chien, A. S., Gygi, S. P. & Nachury, M.  
 47 952 V. (2015). Proteomics of Primary Cilia by Proximity Labeling. *Dev Cell* **35**, 497-512.
- 48 953 62. Chen, C. L., Hu, Y., Udeshi, N. D., Lau, T. Y., Wirtz-Peitz, F., He, L., Ting, A. Y., Carr, S. A. &  
 49 954 Perrimon, N. (2015). Proteomic mapping in live Drosophila tissues using an engineered  
 50 955 ascorbate peroxidase. *Proc Natl Acad Sci U S A* **112**, 12093-8.
- 52 956 63. Lobingier, B. T., Huttenhain, R., Eichel, K., Miller, K. B., Ting, A. Y., von Zastrow, M. & Krogan,  
 53 957 N. J. (2017). An Approach to Spatiotemporally Resolve Protein Interaction Networks in Living  
 54 958 Cells. *Cell* **169**, 350-360 e12.
- 55 959 64. Paek, J., Kalocsay, M., Staus, D. P., Wingler, L., Pascolutti, R., Paulo, J. A., Gygi, S. P. & Kruse,  
 56 960 A. C. (2017). Multidimensional Tracking of GPCR Signaling via Peroxidase-Catalyzed Proximity  
 57 961 Labeling. *Cell* **169**, 338-349 e11.

- 962 65. Loh, K. H., Stawski, P. S., Draycott, A. S., Udeshi, N. D., Lehrman, E. K., Wilton, D. K., Svinkina, T., Deerinck, T. J., Ellisman, M. H., Stevens, B., Carr, S. A. & Ting, A. Y. (2016). Proteomic Analysis of Unbounded Cellular Compartments: Synaptic Clefts. *Cell* **166**, 1295-1307 e21.
- 1 963
- 2 964
- 3 965 66. Kemphues, K. (2000). PARsing embryonic polarity. *Cell* **101**, 345-8.
- 4 966 67. Kemphues, K. J., Priess, J. R., Morton, D. G. & Cheng, N. S. (1988). Identification of genes required for cytoplasmic localization in early *C. elegans* embryos. *Cell* **52**, 311-20.
- 5 967
- 6 968 68. Goldstein, B. & Macara, I. G. (2007). The PAR Proteins: Fundamental Players in Animal Cell Polarization. *Developmental Cell* **13**, 609-622.
- 7 969
- 8 970 69. Huo, Y. & Macara, I. G. (2014). The Par3-like polarity protein Par3L is essential for mammary stem cell maintenance. *Nat Cell Biol* **16**, 529-37.
- 9 971
- 10 972 70. Izumi, Y., Hirose, T., Tamai, Y., Hirai, S., Nagashima, Y., Fujimoto, T., Tabuse, Y., Kemphues, K. J. & Ohno, S. (1998). An atypical PKC directly associates and colocalizes at the epithelial tight junction with ASIP, a mammalian homologue of *Caenorhabditis elegans* polarity protein PAR-3. *J Cell Biol* **143**, 95-106.
- 11 973
- 12 974
- 13 975
- 14 976 71. Brajenovic, M., Joberty, G., Kuster, B., Bouwmeester, T. & Drewes, G. (2004). Comprehensive proteomic analysis of human Par protein complexes reveals an interconnected protein network. *J Biol Chem* **279**, 12804-11.
- 15 977
- 16 978
- 17 979 72. Martin, A. C., Kaschube, M. & Wieschaus, E. F. (2009). Pulsed contractions of an actin-myosin network drive apical constriction. *Nature* **457**, 495-9.
- 18 980
- 19 981 73. Traweger, A., Wiggin, G., Taylor, L., Tate, S. A., Metalnikov, P. & Pawson, T. (2008). Protein phosphatase 1 regulates the phosphorylation state of the polarity scaffold Par-3. *Proc Natl Acad Sci U S A* **105**, 10402-7.
- 20 982
- 21 983
- 22 984 74. Benton, R. & St Johnston, D. (2003). *Drosophila* PAR-1 and 14-3-3 inhibit Bazooka/PAR-3 to establish complementary cortical domains in polarized cells. *Cell* **115**, 691-704.
- 23 985
- 24 986 75. Hurd, T. W., Fan, S., Liu, C. J., Kweon, H. K., Hakansson, K. & Margolis, B. (2003). Phosphorylation-dependent binding of 14-3-3 to the polarity protein Par3 regulates cell polarity in mammalian epithelia. *Curr Biol* **13**, 2082-90.
- 25 987
- 26 988
- 27 989 76. Baas, A. F., Kuipers, J., van der Wel, N. N., Batlle, E., Koerten, H. K., Peters, P. J. & Clevers, H. C. (2004). Complete polarization of single intestinal epithelial cells upon activation of LKB1 by STRAD. *Cell* **116**, 457-66.
- 28 990
- 29 991
- 30 992 77. Sebbagh, M., Santoni, M. J., Hall, B., Borg, J. P. & Schwartz, M. A. (2009). Regulation of LKB1/STRAD localization and function by E-cadherin. *Curr Biol* **19**, 37-42.
- 31 993
- 32 994 78. Lee, J. H., Koh, H., Kim, M., Kim, Y., Lee, S. Y., Karess, R. E., Lee, S. H., Shong, M., Kim, J. M., Kim, J. & Chung, J. (2007). Energy-dependent regulation of cell structure by AMP-activated protein kinase. *Nature* **447**, 1017-20.
- 33 995
- 34 996
- 35 997 79. Wingo, S. N., Gallardo, T. D., Akbay, E. A., Liang, M. C., Contreras, C. M., Boren, T., Shimamura, T., Miller, D. S., Sharpless, N. E., Bardeesy, N., Kwiatkowski, D. J., Schorge, J. O., Wong, K. K. & Castrillon, D. H. (2009). Somatic LKB1 mutations promote cervical cancer progression. *PLoS One* **4**, e5137.
- 36 998
- 37 999
- 38 1000 80. Baas, A. F., Boudeau, J., Sapkota, G. P., Smit, L., Medema, R., Morrice, N. A., Alessi, D. R. & Clevers, H. C. (2003). Activation of the tumour suppressor kinase LKB1 by the STE20-like pseudokinase STRAD. *EMBO J* **22**, 3062-72.
- 39 1001
- 40 1002
- 41 1003
- 42 1004 81. Boudeau, J., Baas, A. F., Deak, M., Morrice, N. A., Kieloch, A., Schutkowski, M., Prescott, A. R., Clevers, H. C. & Alessi, D. R. (2003). MO25alpha/beta interact with STRADalpha/beta enhancing their ability to bind, activate and localize LKB1 in the cytoplasm. *EMBO J* **22**, 5102-14.
- 43 1005
- 44 1006
- 45 1007
- 46 1008 82. Boudeau, J., Deak, M., Lawlor, M. A., Morrice, N. A. & Alessi, D. R. (2003). Heat-shock protein 90 and Cdc37 interact with LKB1 and regulate its stability. *Biochem J* **370**, 849-57.
- 47 1009
- 48 1010 83. Nony, P., Gaude, H., Rossel, M., Fournier, L., Rouault, J. P. & Billaud, M. (2003). Stability of the Peutz-Jeghers syndrome kinase LKB1 requires its binding to the molecular chaperones Hsp90/Cdc37. *Oncogene* **22**, 9165-75.
- 49 1011
- 50 1012
- 51
- 52
- 53
- 54
- 55
- 56
- 57
- 58
- 59
- 60
- 61
- 62
- 63
- 64
- 65

- 1013 84. Jurgens, G., Wieschaus, E., Nusslein-Volhard, C. & Kluding, H. (1984). Mutations affecting the  
11014 pattern of the larval cuticle in *Drosophila melanogaster* : II. Zygotic loci on the third  
21015 chromosome. *Wilehm Roux Arch Dev Biol* **193**, 283-295.
- 31016 85. Tepass, U., Theres, C. & Knust, E. (1990). crumbs encodes an EGF-like protein expressed on  
41017 apical membranes of *Drosophila* epithelial cells and required for organization of epithelia.  
51018 *Cell* **61**, 787-99.
- 71019 86. Bulgakova, N. A. & Knust, E. (2009). The Crumbs complex: from epithelial-cell polarity to  
81020 retinal degeneration. *Journal of Cell Science* **122**, 2587-2596.
- 91021 87. Bachmann, A., Schneider, M., Theilenberg, E., Grawe, F. & Knust, E. (2001). *Drosophila*  
101022 Stardust is a partner of Crumbs in the control of epithelial cell polarity. *Nature* **414**, 638-43.
- 111023 88. Hong, Y., Stronach, B., Perrimon, N., Jan, L. Y. & Jan, Y. N. (2001). *Drosophila* Stardust  
121024 interacts with Crumbs to control polarity of epithelia but not neuroblasts. *Nature* **414**, 634-8.
- 131025 89. Krahn, M. P., Buckers, J., Kastrup, L. & Wodarz, A. (2010). Formation of a Bazooka-Stardust  
151026 complex is essential for plasma membrane polarity in epithelia. *J Cell Biol* **190**, 751-60.
- 161027 90. Morais-de-Sa, E., Mirouse, V. & St Johnston, D. (2010). aPKC phosphorylation of Bazooka  
171028 defines the apical/lateral border in *Drosophila* epithelial cells. *Cell* **141**, 509-23.
- 181029 91. Walther, R. F. & Pichaud, F. (2010). Crumbs/DaPKC-dependent apical exclusion of Bazooka  
191030 promotes photoreceptor polarity remodeling. *Curr Biol* **20**, 1065-74.
- 211031 92. Wodarz, A., Hinz, U., Engelbert, M. & Knust, E. (1995). Expression of crumbs confers apical  
221032 character on plasma membrane domains of ectodermal epithelia of *Drosophila*. *Cell* **82**, 67-  
231033 76.
- 241034 93. Laprise, P., Beronja, S., Silva-Gagliardi, N. F., Pellikka, M., Jensen, A. M., McGlade, C. J. &  
251035 Tepass, U. (2006). The FERM protein Yurt is a negative regulatory component of the Crumbs  
271036 complex that controls epithelial polarity and apical membrane size. *Dev Cell* **11**, 363-74.
- 281037 94. Medina, E., Williams, J., Klipfell, E., Zarnescu, D., Thomas, G. & Le Bivic, A. (2002). Crumbs  
291038 interacts with moesin and beta(Heavy)-spectrin in the apical membrane skeleton of  
301039 *Drosophila*. *J Cell Biol* **158**, 941-51.
- 311040 95. Varelas, X., Samavarchi-Tehrani, P., Narimatsu, M., Weiss, A., Cockburn, K., Larsen, B. G.,  
321041 Rossant, J. & Wrana, J. L. (2010). The Crumbs complex couples cell density sensing to Hippo-  
331042 dependent control of the TGF-beta-SMAD pathway. *Dev Cell* **19**, 831-44.
- 341043 96. Chang, Y., Klezovitch, O., Walikonis, R. S., Vasioukhin, V. & LoTurco, J. J. (2010). Discs large 5  
351044 is required for polarization of citron kinase in mitotic neural precursors. *Cell Cycle* **9**, 1990-7.
- 361045 97. Campbell, C. I., Samavarchi-Tehrani, P., Barrios-Rodiles, M., Datti, A., Gingras, A. C. & Wrana,  
371046 J. L. (2016). The RNF146 and tankyrase pathway maintains the junctional Crumbs complex  
381047 through regulation of angiominin. *J Cell Sci* **129**, 3396-411.
- 391048 98. Zhao, B., Li, L., Lu, Q., Wang, L. H., Liu, C. Y., Lei, Q. & Guan, K. L. (2011). Angiominin is a novel  
401049 Hippo pathway component that inhibits YAP oncoprotein. *Genes Dev* **25**, 51-63.
- 411050 99. Bilder, D., Li, M. & Perrimon, N. (2000). Cooperative regulation of cell polarity and growth by  
421051 *Drosophila* tumor suppressors. *Science* **289**, 113-6.
- 431052 100. Bilder, D., Schober, M. & Perrimon, N. (2003). Integrated activity of PDZ protein complexes  
441053 regulates epithelial polarity. *Nat Cell Biol* **5**, 53-8.
- 451054 101. Albertson, R. & Doe, C. Q. (2003). Dlg, Scrib and Lgl regulate neuroblast cell size and mitotic  
461055 spindle asymmetry. *Nat Cell Biol* **5**, 166-70.
- 471056 102. Huang, L., Kinnucan, E., Wang, G., Beaudenon, S., Howley, P. M., Huibregtse, J. M. &  
481057 Pavletich, N. P. (1999). Structure of an E6AP-UbcH7 complex: insights into ubiquitination by  
491058 the E2-E3 enzyme cascade. *Science* **286**, 1321-6.
- 501059 103. Nakagawa, S. & Huibregtse, J. M. (2000). Human scribble (Vartul) is targeted for ubiquitin-  
511060 mediated degradation by the high-risk papillomavirus E6 proteins and the E6AP ubiquitin-  
521061 protein ligase. *Mol Cell Biol* **20**, 8244-53.
- 531062 104. Lim, K. Y. B., Godde, N. J., Humbert, P. O. & Kvasnakul, M. (2017). Structural basis for the  
541063 differential interaction of Scribble PDZ domains with the guanine nucleotide exchange factor  
551064 beta-PIX. *J Biol Chem* **292**, 20425-20436.
- 561065

- 1065 105. Frank, S. R., Bell, J. H., Frodin, M. & Hansen, S. H. (2012). A betaPIX-PAK2 complex confers protection against Scrib-dependent and cadherin-mediated apoptosis. *Curr Biol* **22**, 1747-54.
- 11066 106. Lahuna, O., Quellarì, M., Achard, C., Nola, S., Meduri, G., Navarro, C., Vitale, N., Borg, J. P. & Misrahi, M. (2005). Thyrotropin receptor trafficking relies on the hScrib-betaPIX-GIT1-ARF6 pathway. *EMBO J* **24**, 1364-74.
- 1067 107. Takizawa, S., Nagasaka, K., Nakagawa, S., Yano, T., Nakagawa, K., Yasugi, T., Takeuchi, T., Kanda, T., Huibregtse, J. M., Akiyama, T. & Taketani, Y. (2006). Human scribble, a novel tumor suppressor identified as a target of high-risk HPV E6 for ubiquitin-mediated degradation, interacts with adenomatous polyposis coli. *Genes Cells* **11**, 453-64.
- 1068 108. Anastas, J. N., Biechele, T. L., Robitaille, M., Muster, J., Allison, K. H., Angers, S. & Moon, R. T. (2012). A protein complex of SCRIB, NOS1AP and VANGL1 regulates cell polarity and migration, and is associated with breast cancer progression. *Oncogene* **31**, 3696-708.
- 1069 109. Cordenosi, M., Zanconato, F., Azzolin, L., Forcato, M., Rosato, A., Frasson, C., Inui, M., Montagner, M., Parenti, A. R., Poletti, A., Daidone, M. G., Dupont, S., Basso, G., Biciato, S. & Piccolo, S. (2011). The Hippo transducer TAZ confers cancer stem cell-related traits on breast cancer cells. *Cell* **147**, 759-72.
- 1070 110. Young, L. C., Hartig, N., Munoz-Alegre, M., Oses-Prieto, J. A., Durdu, S., Bender, S., Vijayakumar, V., Vietri Rudan, M., Gewinner, C., Henderson, S., Jathoul, A. P., Ghatrora, R., Lythgoe, M. F., Burlingame, A. L. & Rodriguez-Viciano, P. (2013). An MRAS, SHOC2, and SCRIB complex coordinates ERK pathway activation with polarity and tumorigenic growth. *Mol Cell* **52**, 679-92.
- 1071 111. Osmani, N., Vitale, N., Borg, J. P. & Etienne-Manneville, S. (2006). Scrib controls Cdc42 localization and activity to promote cell polarization during astrocyte migration. *Curr Biol* **16**, 2395-405.
- 1072 112. Michaelis, U. R., Chavakis, E., Kruse, C., Jungblut, B., Kaluza, D., Wandzioch, K., Manavski, Y., Heide, H., Santoni, M. J., Potente, M., Eble, J. A., Borg, J. P. & Brandes, R. P. (2013). The polarity protein Scrib is essential for directed endothelial cell migration. *Circ Res* **112**, 924-34.
- 1073 113. Nola, S., Sebbagh, M., Marchetto, S., Osmani, N., Nourry, C., Audebert, S., Navarro, C., Rachel, R., Montcouquiol, M., Sans, N., Etienne-Manneville, S., Borg, J. P. & Santoni, M. J. (2008). Scrib regulates PAK activity during the cell migration process. *Hum Mol Genet* **17**, 3552-65.
- 1074 114. Chen, B., Zheng, B., DeRan, M., Jarugumilli, G. K., Fu, J., Brooks, Y. S. & Wu, X. (2016). ZDHHC7-mediated S-palmitoylation of Scribble regulates cell polarity. *Nat Chem Biol* **12**, 686-93.
- 1075 115. Legouis, R., Jaulin-Bastard, F., Schott, S., Navarro, C., Borg, J. P. & Labouesse, M. (2003). Basolateral targeting by leucine-rich repeat domains in epithelial cells. *EMBO Rep* **4**, 1096-102.
- 1076 116. Navarro, C., Nola, S., Audebert, S., Santoni, M. J., Arsanto, J. P., Ginestier, C., Marchetto, S., Jacquemier, J., Isnardon, D., Le Bivic, A., Birnbaum, D. & Borg, J. P. (2005). Junctional recruitment of mammalian Scribble relies on E-cadherin engagement. *Oncogene* **24**, 4330-9.
- 1077 117. Feigin, M. E., Akshinthala, S. D., Araki, K., Rosenberg, A. Z., Muthuswamy, L. B., Martin, B., Lehmann, B. D., Berman, H. K., Pietenpol, J. A., Cardiff, R. D. & Muthuswamy, S. K. (2014). Mislocalization of the cell polarity protein scribble promotes mammary tumorigenesis and is associated with basal breast cancer. *Cancer Res* **74**, 3180-94.
- 1078 118. Humbert, P. O., Grzeschik, N. A., Brumby, A. M., Galea, R., Elsum, I. & Richardson, H. E. (2008). Control of tumorigenesis by the Scribble/Dlg/Lgl polarity module. *Oncogene* **27**, 6888-907.
- 1079 119. Zhan, L., Rosenberg, A., Bergami, K. C., Yu, M., Xuan, Z., Jaffe, A. B., Allred, C. & Muthuswamy, S. K. (2008). Dereglulation of scribble promotes mammary tumorigenesis and reveals a role for cell polarity in carcinoma. *Cell* **135**, 865-78.
- 1080 1081 1082 1083 1084 1085 1086 1087 1088 1089 1090 1091 1092 1093 1094 1095 1096 1097 1098 1099 1100 1101 1102 1103 1104 1105 1106 1107 1108 1109 1110 1111 1112 1113 1114

- 1115 120. Dow, L. E., Elsum, I. A., King, C. L., Kinross, K. M., Richardson, H. E. & Humbert, P. O. (2008). Loss of human Scribble cooperates with H-Ras to promote cell invasion through deregulation of MAPK signalling. *Oncogene* **27**, 5988-6001.
- 11116
- 21117
- 31118 121. Hawkins, E. D., Oliaro, J., Ramsbottom, K. M., Newbold, A., Humbert, P. O., Johnstone, R. W. & Russell, S. M. (2016). Scribble acts as an oncogene in Emu-myc-driven lymphoma. *Oncogene* **35**, 1193-7.
- 41119
- 51120
- 61121 122. Kuo, J. C., Han, X., Hsiao, C. T., Yates, J. R., 3rd & Waterman, C. M. (2011). Analysis of the myosin-II-responsive focal adhesion proteome reveals a role for beta-Pix in negative regulation of focal adhesion maturation. *Nat Cell Biol* **13**, 383-93.
- 71122
- 81123
- 91124 123. Horton, E. R., Byron, A., Askari, J. A., Ng, D. H., Millon-Fremillon, A., Robertson, J., Koper, E. J., Paul, N. R., Warwood, S., Knight, D., Humphries, J. D. & Humphries, M. J. (2015). Definition of a consensus integrin adhesome and its dynamics during adhesion complex assembly and disassembly. *Nat Cell Biol* **17**, 1577-87.
- 101125
- 111126
- 121127
- 131128 124. Schiller, H. B., Friedel, C. C., Boulegue, C. & Fassler, R. (2011). Quantitative proteomics of the integrin adhesome show a myosin II-dependent recruitment of LIM domain proteins. *EMBO Rep* **12**, 259-66.
- 141129
- 151130
- 161131 125. Schiller, H. B., Hermann, M. R., Polleux, J., Vignaud, T., Zanivan, S., Friedel, C. C., Sun, Z., Raducanu, A., Gottschalk, K. E., Thery, M., Mann, M. & Fassler, R. (2013). beta1- and alphaV-class integrins cooperate to regulate myosin II during rigidity sensing of fibronectin-based microenvironments. *Nat Cell Biol* **15**, 625-36.
- 171132
- 181133
- 191134
- 201135 126. Gubb, D. & Garcia-Bellido, A. (1982). A genetic analysis of the determination of cuticular polarity during development in *Drosophila melanogaster*. *J Embryol Exp Morphol* **68**, 37-57.
- 211136
- 221137 127. Chiu, C. W., Monat, C., Robitaille, M., Lacomme, M., Daulat, A. M., Macleod, G., McNeill, H., Cayouette, M. & Angers, S. (2016). SAPCD2 Controls Spindle Orientation and Asymmetric Divisions by Negatively Regulating the Galphai-LGN-NuMA Ternary Complex. *Dev Cell* **36**, 50-62.
- 231138
- 241139
- 251140
- 261141 128. Zhang, L., Luga, V., Armitage, S. K., Musiol, M., Won, A., Yip, C. M., Plotnikov, S. V. & Wrana, J. L. (2016). A lateral signalling pathway coordinates shape volatility during cell migration. *Nat Commun* **7**, 11714.
- 271142
- 281143
- 291144 129. Paricio, N., Feiguin, F., Boutros, M., Eaton, S. & Mlodzik, M. (1999). The *Drosophila* STE20-like kinase misshapen is required downstream of the Frizzled receptor in planar polarity signaling. *EMBO J* **18**, 4669-78.
- 301145
- 311146
- 321147 130. Lee, R. H., Iioka, H., Ohashi, M., Iemura, S., Natsume, T. & Kinoshita, N. (2007). XRab40 and XCullin5 form a ubiquitin ligase complex essential for the noncanonical Wnt pathway. *EMBO J* **26**, 3592-606.
- 331148
- 341149
- 351150 131. Daulat, A. M., Bertucci, F., Audebert, S., Serge, A., Finetti, P., Josselin, E., Castellano, R., Birnbaum, D., Angers, S. & Borg, J. P. (2016). PRICKLE1 Contributes to Cancer Cell Dissemination through Its Interaction with mTORC2. *Dev Cell* **37**, 311-25.
- 361151
- 371152
- 381153 132. Lim, B. C., Matsumoto, S., Yamamoto, H., Mizuno, H., Kikuta, J., Ishii, M. & Kikuchi, A. (2016). Prickle1 promotes focal adhesion disassembly in cooperation with the CLASP-LL5beta complex in migrating cells. *J Cell Sci* **129**, 3115-29.
- 391154
- 401155
- 411156 133. Daulat, A. M. & Borg, J. P. (2016). When mTORC2-AKT signaling meets cell polarity. *Cell Cycle*, 1-2.
- 421157
- 431158 134. Zhang, L. & Wrana, J. L. (2016). Regulation of Rho GTPases from the lateral sides of migrating cells. *Small GTPases*, 1-4.
- 441159
- 451160 135. Montcouquiol, M., Rachel, R. A., Lanford, P. J., Copeland, N. G., Jenkins, N. A. & Kelley, M. W. (2003). Identification of Vangl2 and Scrb1 as planar polarity genes in mammals. *Nature* **423**, 173-7.
- 461161
- 471162
- 481163 136. Sun, T., Yang, L., Kaur, H., Pestel, J., Looso, M., Nolte, H., Krasel, C., Heil, D., Krishnan, R. K., Santoni, M. J., Borg, J. P., Bunemann, M., Offermanns, S., Swiercz, J. M. & Worzfeld, T. (2017). A reverse signaling pathway downstream of Sema4A controls cell migration via Scrib. *J Cell Biol* **216**, 199-215.
- 491165
- 501166
- 51
- 52
- 53
- 54
- 55
- 56
- 57
- 58
- 59
- 60
- 61
- 62
- 63
- 64
- 65

- 1167 137. Bastock, R., Strutt, H. & Strutt, D. (2003). Strabismus is asymmetrically localised and binds to Prickle and Dishevelled during Drosophila planar polarity patterning. *Development* **130**, 3007-14.
- 1168
- 21169
- 31170 138. Rawls, A. S. & Wolff, T. (2003). Strabismus requires Flamingo and Prickle function to regulate tissue polarity in the Drosophila eye. *Development* **130**, 1877-87.
- 41171
- 51172 139. Jenny, A., Darken, R. S., Wilson, P. A. & Mlodzik, M. (2003). Prickle and Strabismus form a functional complex to generate a correct axis during planar cell polarity signaling. *EMBO J* **22**, 4409-20.
- 71173
- 81174
- 91175 140. Temkin, P., Lauffer, B., Jager, S., Cimermancic, P., Krogan, N. J. & von Zastrow, M. (2011). SNX27 mediates retromer tubule entry and endosome-to-plasma membrane trafficking of signalling receptors. *Nat Cell Biol* **13**, 715-21.
- 101176
- 111177
- 121178 141. Belotti, E., Puvirajesinghe, T. M., Audebert, S., Baudalet, E., Camoin, L., Pierres, M., Lasvaux, L., Ferracci, G., Montcouquiol, M. & Borg, J. P. (2012). Molecular characterisation of endogenous Vangl2/Vangl1 heteromeric protein complexes. *PLoS One* **7**, e46213.
- 141179
- 151180
- 161181 142. Lu, X., Borchers, A. G., Jolicoeur, C., Rayburn, H., Baker, J. C. & Tessier-Lavigne, M. (2004). PTK7/CCK-4 is a novel regulator of planar cell polarity in vertebrates. *Nature* **430**, 93-8.
- 171182
- 181183 143. Lhoumeau, A. C., Puppo, F., Prebet, T., Kodjabachian, L. & Borg, J. P. (2011). PTK7: a cell polarity receptor with multiple facets. *Cell Cycle* **10**, 1233-6.
- 201184
- 211185 144. Wehner, P., Shnitsar, I., Urlaub, H. & Borchers, A. (2011). RACK1 is a novel interaction partner of PTK7 that is required for neural tube closure. *Development* **138**, 1321-7.
- 221186
- 231187 145. Li, S., Esterberg, R., Lachance, V., Ren, D., Radde-Gallwitz, K., Chi, F., Parent, J. L., Fritz, A. & Chen, P. (2011). Rack1 is required for Vangl2 membrane localization and planar cell polarity signaling while attenuating canonical Wnt activity. *Proc Natl Acad Sci U S A* **108**, 2264-9.
- 241188
- 251189
- 271190 146. Reiter, J. F. & Leroux, M. R. (2017). Genes and molecular pathways underpinning ciliopathies. *Nat Rev Mol Cell Biol* **18**, 533-547.
- 281191
- 291192 147. Ostrowski, L. E., Blackburn, K., Radde, K. M., Moyer, M. B., Schlatzer, D. M., Moseley, A. & Boucher, R. C. (2002). A proteomic analysis of human cilia: identification of novel components. *Mol Cell Proteomics* **1**, 451-65.
- 301193
- 311194
- 321195 148. Liu, Q., Tan, G., Levenkova, N., Li, T., Pugh, E. N., Jr., Rux, J. J., Speicher, D. W. & Pierce, E. A. (2007). The proteome of the mouse photoreceptor sensory cilium complex. *Mol Cell Proteomics* **6**, 1299-317.
- 341196
- 351197
- 361198 149. Ishikawa, H., Thompson, J., Yates, J. R., 3rd & Marshall, W. F. (2012). Proteomic analysis of mammalian primary cilia. *Curr Biol* **22**, 414-9.
- 371199
- 381199
- 391200 150. Jakobsen, L., Vanselow, K., Skogs, M., Toyoda, Y., Lundberg, E., Poser, I., Falkenby, L. G., Bennetzen, M., Westendorf, J., Nigg, E. A., Uhlen, M., Hyman, A. A. & Andersen, J. S. (2011). Novel asymmetrically localizing components of human centrosomes identified by complementary proteomics methods. *EMBO J* **30**, 1520-35.
- 401201
- 411202
- 421203 151. Borovina, A., Superina, S., Voskas, D. & Ciruna, B. (2010). Vangl2 directs the posterior tilting and asymmetric localization of motile primary cilia. *Nat Cell Biol* **12**, 407-12.
- 431204
- 441205
- 451206 152. May-Simera, H. L., Petralia, R. S., Montcouquiol, M., Wang, Y. X., Szarama, K. B., Liu, Y., Lin, W., Deans, M. R., Pazour, G. J. & Kelley, M. W. (2015). Ciliary proteins Bbs8 and Ift20 promote planar cell polarity in the cochlea. *Development* **142**, 555-66.
- 471207
- 481208
- 491209 153. Omori, Y., Zhao, C., Saras, A., Mukhopadhyay, S., Kim, W., Furukawa, T., Sengupta, P., Veraksa, A. & Malicki, J. (2008). Elipsa is an early determinant of ciliogenesis that links the IFT particle to membrane-associated small GTPase Rab8. *Nat Cell Biol* **10**, 437-44.
- 501210
- 511211
- 521212 154. Liew, G. M., Ye, F., Nager, A. R., Murphy, J. P., Lee, J. S., Aguiar, M., Breslow, D. K., Gygi, S. P. & Nachury, M. V. (2014). The intraflagellar transport protein IFT27 promotes BBSome exit from cilia through the GTPase ARL6/BBS3. *Dev Cell* **31**, 265-78.
- 541213
- 551214
- 561215 155. Soderberg, O., Gullberg, M., Jarvius, M., Ridderstrale, K., Leuchowius, K. J., Jarvius, J., Wester, K., Hydbring, P., Bahram, F., Larsson, L. G. & Landegren, U. (2006). Direct observation of individual endogenous protein complexes in situ by proximity ligation. *Nat Methods* **3**, 995-1000.
- 581216
- 591217
- 601218
- 61
- 62
- 63
- 64
- 65

- 1219 156. Smith, M. A., Hall, R., Fisher, K., Haake, S. M., Khalil, F., Schabath, M. B., Vuaroqueaux, V.,  
11220 Fiebig, H. H., Altiok, S., Chen, Y. A. & Haura, E. B. (2015). Annotation of human cancers with  
12221 EGFR signaling-associated protein complexes using proximity ligation assays. *Sci Signal* **8**, ra4.  
1222 157. Roncagalli, R., Cucchetti, M., Jarmuzynski, N., Gregoire, C., Bergot, E., Audebert, S., Baudelet,  
1223 E., Menoita, M. G., Joachim, A., Durand, S., Suchanek, M., Fiore, F., Zhang, L., Liang, Y.,  
1224 Camoin, L., Malissen, M. & Malissen, B. (2016). The scaffolding function of the RLTPR protein  
1225 explains its essential role for CD28 co-stimulation in mouse and human T cells. *J Exp Med*  
1226 **213**, 2437-2457.  
1227 158. Bar, D. Z., Atkash, K., Tavarez, U., Erdos, M. R., Gruenbaum, Y. & Collins, F. S. (2018).  
1228 Biotinylation by antibody recognition-a method for proximity labeling. *Nat Methods* **15**, 127-  
1229 133.  
1230 159. Kim, D. I., Cutler, J. A., Na, C. H., Reckel, S., Renuse, S., Madugundu, A. K., Tahir, R.,  
1231 Goldschmidt, H. L., Reddy, K. L., Haganir, R. L., Wu, X., Zachara, N. E., Hantschel, O. & Pandey,  
1232 A. (2018). BioSITE: A Method for Direct Detection and Quantitation of Site-Specific  
1233 Biotinylation. *J Proteome Res* **17**, 759-769.  
1234 160. Udeshi, N. D., Pedram, K., Svinikina, T., Fereshetian, S., Myers, S. A., Aygun, O., Krug, K.,  
1235 Clauser, K., Ryan, D., Ast, T., Mootha, V. K., Ting, A. Y. & Carr, S. A. (2017). Antibodies to  
1236 biotin enable large-scale detection of biotinylation sites on proteins. *Nat Methods* **14**, 1167-  
1237 1170.  
1238 161. Xie, J., Han, M., Zhang, M., Deng, H. & Wu, W. (2018). PP5 (PPP5C) is a phosphatase of Dvl2.  
1239 *Sci Rep* **8**, 2715.  
1240 162. Yoshihara, K., Ikenouchi, J., Izumi, Y., Akashi, M., Tsukita, S. & Furuse, M. (2011).  
1241 Phosphorylation state regulates the localization of Scribble at adherens junctions and its  
1242 association with E-cadherin-catenin complexes. *Exp Cell Res* **317**, 413-22.  
1243 163. Hardmanmm, G., Perkins, S., Ruan, Z., Kannan, N., Brownridge, P., Byrne, D. P., Evers, P. A.,  
1244 Jones, A. R. & Evers, C., E. (2017). Extensive non-canonical phosphorylation in human cells  
1245 revealed using strong-anion exchange-mediated phosphoproteomics. In *bioRxiv preprint*.  
1246 bioRxiv preprint.

## Figure legends

Figure 1: Key features of the epithelial polarity program

A) Schematic representation of the Apico-Basal Polarity (ABP) and Planar Cell Polarity (PCP) processes. B) Subcellular localization of prototypic ABP proteins, Crumb, PAR and SCRIB protein complexes, indicating their reciprocal inhibition. C) Subcellular localization of PCP proteins in the *Drosophila* wing epithelium showing their asymmetric localization at either the proximal or distal cell membranes.

Figure 2: Main steps of MS sample preparation and analysis

1257 Complex protein samples derived from tissues or cultured cell lines are fractionated  
1  
21258 and purified for mass spectrometry analysis. Proteins can be subjected to separation  
3  
4  
51259 with acrylamide gels or processed directly (shotgun proteomics). Enzymatic digestion  
6  
71260 can be used to generate peptides, which can be separated and individually analyzed  
8  
9  
101261 using the mass spectrometer. Search engines are used to analyze the generated  
11  
121262 data for each peptide and compared to information available from different protein  
13  
141263 databases, which allows the identification of proteins.  
15

16  
17  
181264  
19  
20  
21  
221265 Figure 3: Key findings from MS-based studies revealing the underlying cellular  
23  
241266 mechanisms of action of the PAR protein complex

25  
26  
27  
281267 Subcellular localization of PAR-4/LKB1 and PAR-3, members of the PAR protein  
29  
301268 complex. MO25 is needed to fully activate LKB1 and for its interaction with either  
31  
32  
331269 STRAD- $\alpha$  or STRAD- $\beta$  and consequent signaling activity. PAR-4/LKB1 activity is  
34  
351270 stabilized following interaction with CDC37 and HSP90. Proteomic approaches have  
36  
37  
381271 identified the PAR-4/LKB1 complex in the primary cilia of epithelial cells. The PAR-3  
39  
401272 complex is localized at the apical side of epithelial cells and is phosphorylated by  
41  
42  
431273 PAR-1 which in turn liberates aPKC and promotes 14-3-3 binding. PP1  
44  
451274 dephosphorylates PAR-3 and restores PAR-3 association with aPKC.

46  
47  
48  
491275  
50  
51  
521276 Figure 4: Role of the SCRIB complex in epithelial polarity and cell migration

53  
54  
55  
561277 Basolaterally-localized SCRIB is associated with the highlighted proteins and acts to  
57  
58  
591278 decrease AKT, HIPPO and ERK signaling. In migrating cells, SCRIB is localized at

60  
61  
62  
63  
64  
65

1279 the leading edge of migrating cells and promotes activation of small G-proteins  
1  
21280 (RAC1, CDC42 or ARF6) in order to enhance cell motility.  
3  
4  
5

61281

7

8

9

101282 Figure 5: Mass spectrometry-based analysis of the SCRIB protein complex

11

12

131283 Schematic representation of the result of successive proteomics approaches used to

14

15 identify protein complexes associated with SCRIB. Each dashed circle encompasses

161284

17

181285 proteins identified by different experimental approaches. Cross-validation of known

19

201286 SCRIB-associated proteins has been possible as well as the elucidation of novel

21

22

231287 components of the SCRIB protein complex.  
24  
25  
26

271288

28

29

30

311289 Figure 6: Mechanistic insights into the roles of VANGL and PRICKLE1 during cancer  
32

331290

34

35

36

371291 VANGL-1/-2 and PRICKLE1 are localized at the leading edge of migratory cancer  
38

391292

40

411293 contribute to cell migration by decreasing RhoA activation, increasing AKT signaling  
42

43

441294 and remodeling focal adhesions. VANGL2 associates with p62/SQSTM1 in  
45

461295

47

48

49

501296

51

52

53

541297

55

561298

57

58

59

601299

61

62

63

64

65

Table 1:

<i>Experimental Approach</i>	<i>Main features</i>	<i>Major limitations</i>
Peptide Pull-down	Based on chemically synthesized peptides; allows the purification of protein complexes from diverse origins (cultured cells or tissues); current method of choice for determining protein-protein interactions; different immobilization techniques are applicable (covalent interactions using biotinylation and non-covalent interactions employing 6x His or GST-tags).	Solubility and size render certain synthetic peptides incompatible with this experimental procedure.
Tandem Affinity Purification	Successfully applied in the purification of membrane protein complexes; associated with low levels of non-specific protein binding.	Potential spatial interference or non-specific protein binding with protein tags (false positives may be detected); lengthy two-step purification protocol may lead to the loss of low affinity proteins.
Single-Step purification	Successfully applied in the purification of membrane and cytosolic protein complexes; straight-forward one-step purification protocol.	Potential spatial interference or non-specific binding with protein tag (false positives may be detected); high rate of background protein binding.
Endogenous Immunoprecipitation	Purification of endogenous complexes is possible; associated with a low rate of false positives.	Reliance on high-affinity antibodies and good expression levels of endogenous proteins.
BioID	Applied to purify proteins in the neighbourhood of a protein of interest; successfully used to identify low-affinity protein-protein interactions.	Protein identification may include proteins in the close spatial neighbourhood of the given protein of interest and not necessarily strongly associated with the protein of interest; protein labelling can occur during all stages of protein turnover of the given protein of interest.
APEX	Used to purify proteins in the neighbourhood of a protein of interest; used to identify low affinity protein-protein interactions; purification of proteins deriving from a specific subcellular compartment is possible; spatiotemporal identification of protein complexes is possible.	Protein identification may include proteins in the close spatial neighbourhood of the given protein of interest and not necessarily associated with the protein of interest.

FIGURE 1: Key features of the epithelial polarity programm

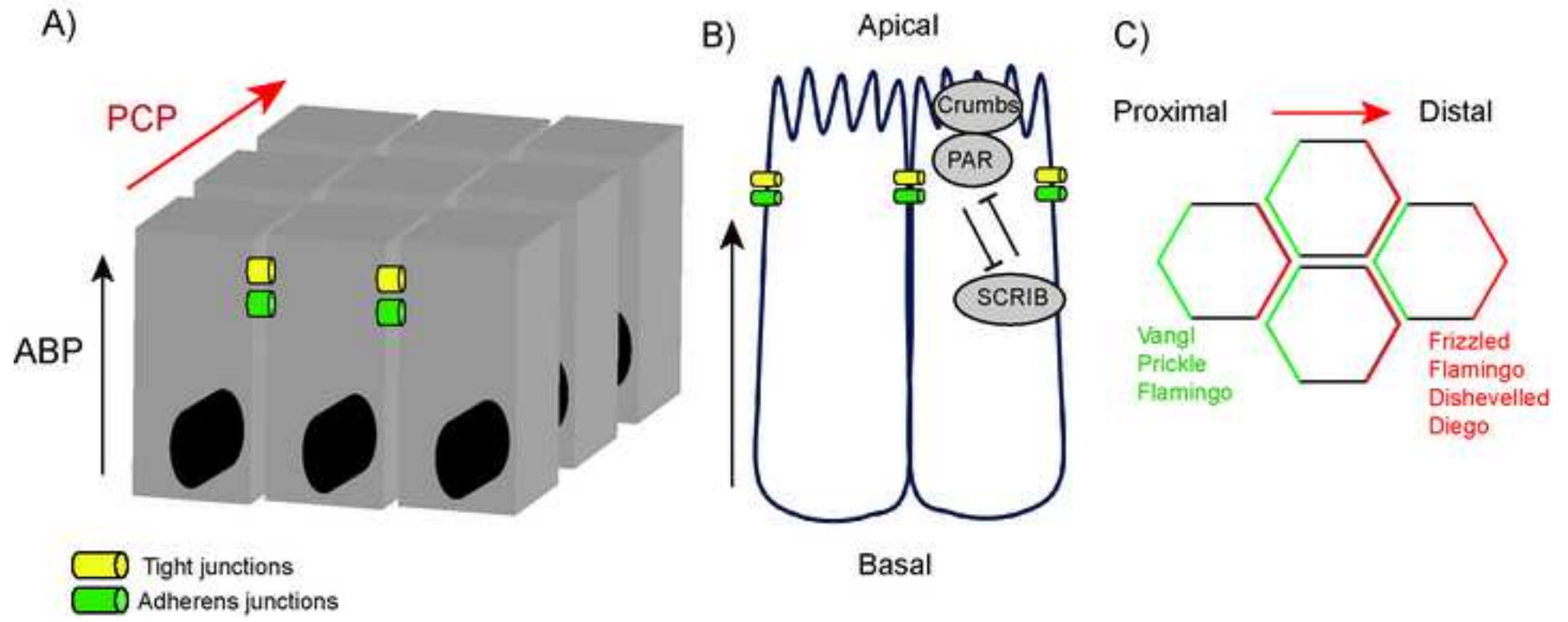


Figure2

[Click here to download high resolution image](#)

FIGURE 2: Pipeline of mass spectrometry sample preparation

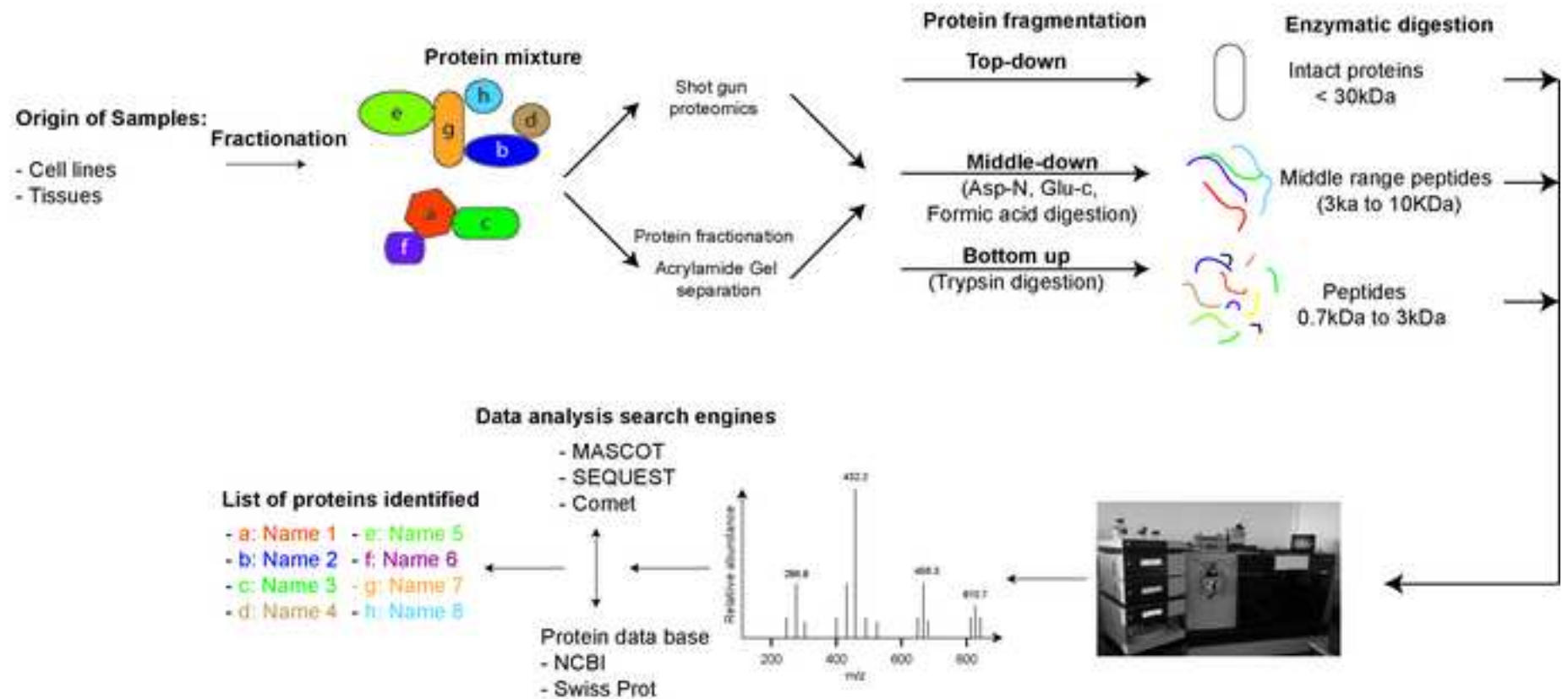


Figure3

[Click here to download high resolution image](#)

FIGURE 3: Key findings from MS-based studies revealing the underlying cellular mechanisms of the PAR protein complex

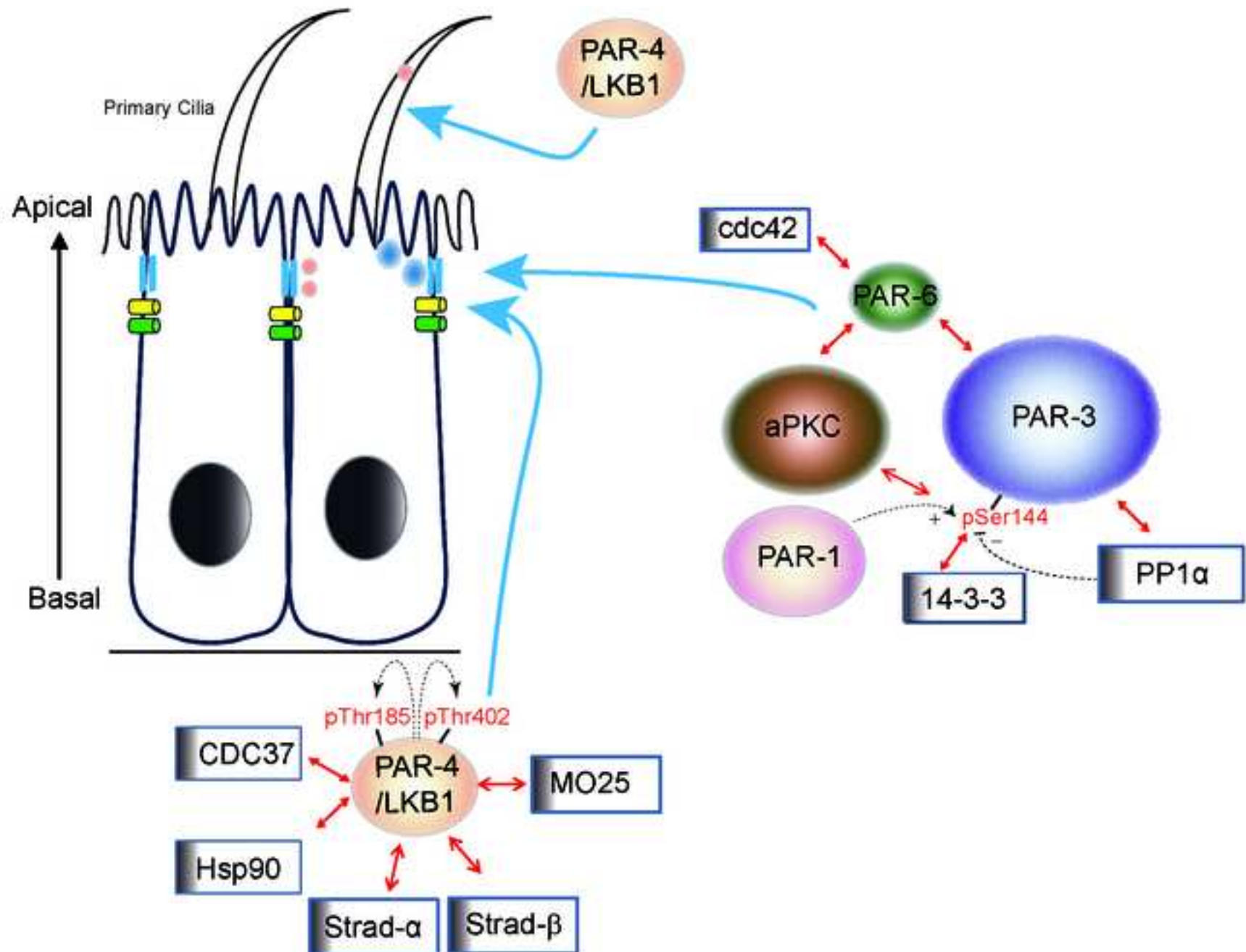


FIGURE 4: Role of the SCRIB complex in epithelial polarity and cell migration

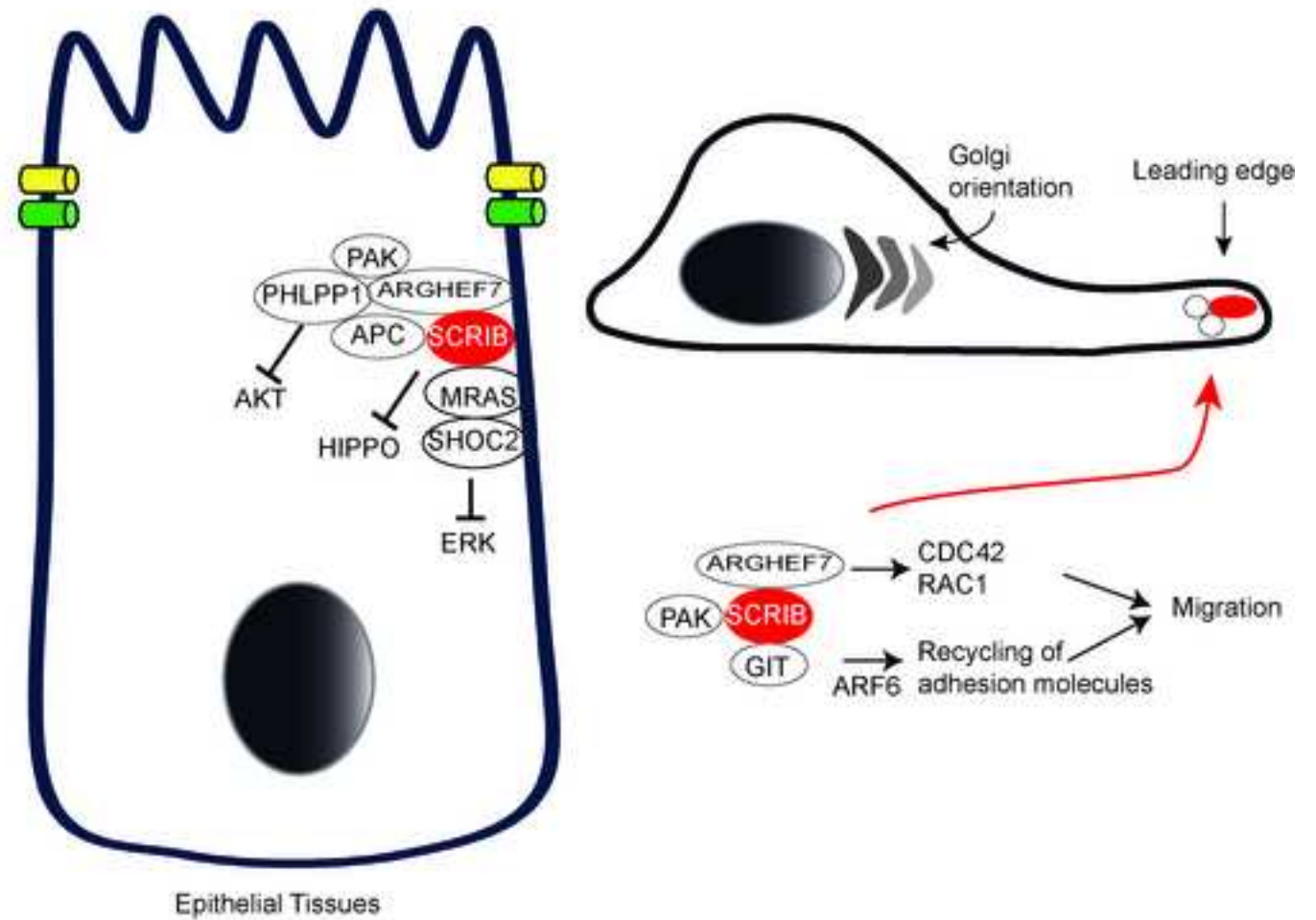


Figure5

[Click here to download high resolution image](#)

FIGURE 5: Mass spectrometry-based analysis of the SCRIB protein complex

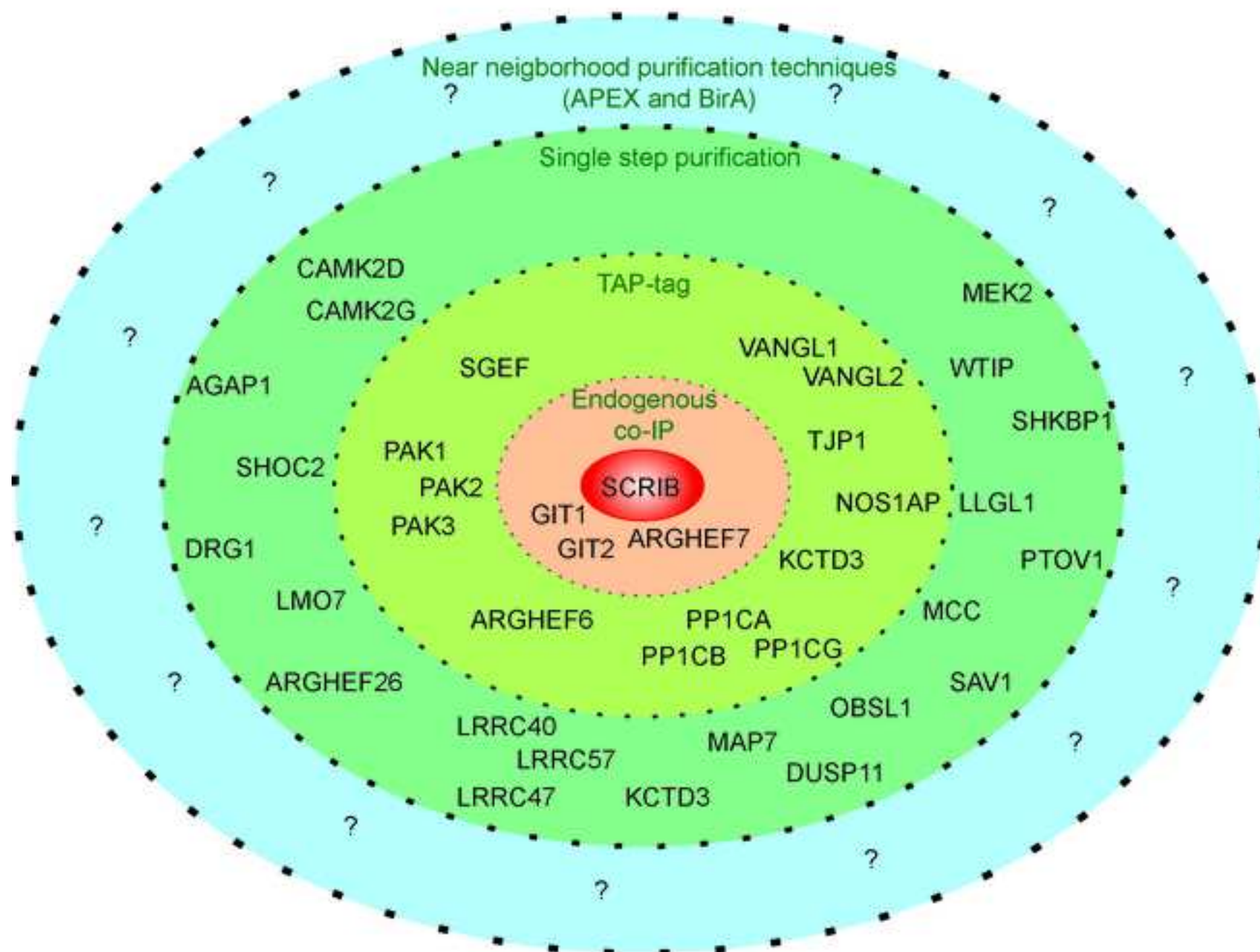


FIGURE 6: Mechanistic insights into the roles of VANGL and PRICKLE1 during cancer cell progression

